

# *Challenges in quantifying changes in the global water cycle*

Article

Accepted Version

Hegerl, G. C., Black, E. ORCID: <https://orcid.org/0000-0003-1344-6186>, Allan, R. P. ORCID: <https://orcid.org/0000-0003-0264-9447>, Ingram, W. J., Polson, D., Trenberth, K. E., Chadwick, R. S., Arkin, P. A., Sarojini, B. B., Becker, A., Dai, A., Durack, P. J., Easterling, D., Fowler, H. J., Kendon, E. J., Huffman, G. J., Liu, C., Marsh, R., New, M., Osborn, T. J., Skliris, N., Stott, P. A., Vidale, P.-L. ORCID: <https://orcid.org/0000-0002-1800-8460>, Wijnffels, S. E., Wilcox, L. J. ORCID: <https://orcid.org/0000-0001-5691-1493>, Willett, K. M. and Zhang, X. (2015) Challenges in quantifying changes in the global water cycle. *Bulletin of the American Meteorological Society*, 96 (7). pp. 1097-1115. ISSN 1520-0477 doi: <https://doi.org/10.1175/BAMS-D-13-00212.1>  
Available at <https://centaur.reading.ac.uk/38063/>

It is advisable to refer to the publisher's version if you intend to cite from the work. See [Guidance on citing](#).

Published version at: <http://journals.ametsoc.org/doi/abs/10.1175/BAMS-D-13-00212.1>

To link to this article DOI: <http://dx.doi.org/10.1175/BAMS-D-13-00212.1>

Publisher: American Meteorological Society

including copyright law. Copyright and IPR is retained by the creators or other copyright holders. Terms and conditions for use of this material are defined in the [End User Agreement](#).

[www.reading.ac.uk/centaur](http://www.reading.ac.uk/centaur)

## **CentAUR**

Central Archive at the University of Reading

Reading's research outputs online



# AMERICAN METEOROLOGICAL SOCIETY

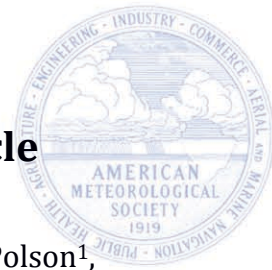
*Bulletin of the American Meteorological Society*

## **EARLY ONLINE RELEASE**

This is a preliminary PDF of the author-produced manuscript that has been peer-reviewed and accepted for publication. Since it is being posted so soon after acceptance, it has not yet been copyedited, formatted, or processed by AMS Publications. This preliminary version of the manuscript may be downloaded, distributed, and cited, but please be aware that there will be visual differences and possibly some content differences between this version and the final published version.

The DOI for this manuscript is doi: [10.1175/BAMS-D-13-00212.1](https://doi.org/10.1175/BAMS-D-13-00212.1)

The final published version of this manuscript will replace the preliminary version at the above DOI once it is available.



# 1 Challenges in quantifying changes in the global water cycle

2 Gabriele C. Hegerl<sup>1</sup>, Emily Black<sup>2</sup>, Richard P. Allan<sup>2</sup>, William J. Ingram<sup>3,4</sup>, Debbie Polson<sup>1</sup>,  
3 Kevin E. Trenberth<sup>5</sup>, Robin S. Chadwick<sup>3</sup>, Phillip A. Arkin<sup>6</sup>, Beena Balan Sarojini<sup>2</sup>,  
4 Andreas Becker<sup>7</sup>, Aiguo Dai<sup>8,5</sup>, Paul J. Durack<sup>9,16</sup>, David Easterling<sup>10</sup>, Hayley J. Fowler<sup>11</sup>,  
5 Elizabeth J. Kendon<sup>3</sup>, George J. Huffman<sup>12</sup>, Chunlei Liu<sup>2</sup>, Robert Marsh<sup>13</sup>, Mark New<sup>14</sup>,  
6 Timothy J. Osborn<sup>15</sup>, Nikolaos Skliris<sup>13</sup>, Peter A. Stott<sup>3</sup>, Pier-Luigi Vidale<sup>2</sup>, Susan E.  
7 Wijffels<sup>16</sup>, Laura J. Wilcox<sup>2</sup>, Kate M. Willett<sup>3</sup>, Xuebin Zhang<sup>17</sup>

8 1. School of GeoSciences, University of Edinburgh, Grant Institute, Kings Buildings, UK EH9  
9 3JW.

10 2. Department of Meteorology, University of Reading/NCAS Climate

11 3. Met Office Hadley Centre, Exeter, UK.

12 4. Department of Physics, Oxford University, Oxford, UK

13 5. NCAR, Boulder, CO, USA.

14 6. ESSIC, University of Maryland, College Park, College Park, MD

15 7. Deutscher Wetterdienst, Offenbach, Germany

16 8. Department of Atmospheric and Environmental Sciences, University at Albany, SUNY,  
17 Albany, NY, USA.

18 9. Program for Climate Model Diagnosis and Intercomparison, Lawrence Livermore  
19 National Laboratory, California, USA.

20 10. NOAA/National Climatic Data Center, Asheville, NC.

21 11. School of Civil Engineering and Geosciences, Newcastle University, UK.

22 12. NASA Goddard Space Flight Center, Greenbelt, MD, USA.

23 13. Ocean and Earth Science, University of Southampton, UK

24 14. University of Cape Town, South Africa.

25 15. Climatic Research Unit, School of Environmental Sciences, University of East Anglia, UK.

26 16. Commonwealth Scientific and Industrial Research Organisation (CSIRO), Tasmania,  
27 Australia.

28 17. Climate Research Division, Environment Canada, Canada.  
29

30 **Corresponding Author:** Gabriele Hegerl, [gabi.hegerl@ed.ac.uk](mailto:gabi.hegerl@ed.ac.uk), GeoSciences, Grant Institute,  
31 Kings Buildings, W Mains Rd, Edinburgh, EH9 3JW, UK

32 **CAPSULE (35 words):**

33 **Human influences have likely already impacted the large-scale water cycle but**  
34 **natural variability and observational uncertainty are substantial. It is essential to**  
35 **maintain and improve observational capabilities to better characterize changes.**

36

37 **Abstract**

38 Understanding observed changes to the global water cycle is key to predicting future  
39 climate changes and their impacts. While many datasets document crucial variables  
40 such as precipitation, ocean salinity, runoff, and humidity, most are uncertain for  
41 determining long-term changes. In situ networks provide long time-series over land but  
42 are sparse in many regions, particularly the tropics. Satellite and reanalysis datasets  
43 provide global coverage, but their long-term stability is lacking. However, comparisons  
44 of changes among related variables can give insights into the robustness of observed  
45 changes. For example, ocean salinity, interpreted with an understanding of ocean  
46 processes, can help cross-validate precipitation. Observational evidence for human  
47 influences on the water cycle is emerging, but uncertainties resulting from internal  
48 variability and observational errors are too large to determine whether the observed  
49 and simulated changes are consistent. Improvements to the in situ and satellite  
50 observing networks that monitor the changing water cycle are required, yet continued  
51 data coverage is threatened by funding reductions. Uncertainty both in the role of  
52 anthropogenic aerosols, and due to large climate variability presently limits confidence  
53 in attribution of observed changes.

## 54 **1. Introduction**

55 Climate change, alongside increased demand for water (World Water Development  
56 Report 2003; WHO/UNICEF 2011), is projected to increase water scarcity in many  
57 regions over the next few decades (e.g., Arnell et al. 2013; Kundzewicz et al. 2007).  
58 Extremes linked to the water cycle, such as droughts, heavy rainfall and floods, already  
59 cause substantial damage (e.g. Lazo et al. 2011; Peterson et al., 2012; 2013) and such  
60 events are expected to increase in severity and frequency (Dai 2011a, 2013a; IPCC  
61 2012, Collins et al. 2013a).

62 Better management of water resources and adaptation to expected changes require  
63 reliable predictions of the water cycle. Such predictions must be grounded in the  
64 changes already observed. This requires quantification of long-term large-scale changes  
65 in key water cycle variables, and estimation of the contribution from natural climate  
66 variability and external forcings, including through studies that are referred to as  
67 detection and attribution (see Stott et al., 2010; Hegerl and Zwiers 2011). Successful  
68 examples of detection and attribution are reported in Bindoff et al. (2013).

69 We discuss how well the available observing capability can capture expected changes in  
70 the global water cycle, including the increasing water content of the atmosphere,  
71 strengthening of climatological precipitation minus evaporation (P-E) patterns, the  
72 pronounced spatial structure and sharp gradients in precipitation change, and increases  
73 of extreme precipitation. We also discuss the challenges inherent in combining an  
74 incomplete observational record with imperfect climate models, to detect  
75 anthropogenic changes in the water cycle.

76 Drawing on discussions from a workshop held at the University of Reading, U.K. in June  
77 2012, we focus on long-term large-scale changes in a few key variables that are both  
78 potentially related to climate change, and essential for diagnosing changes in the global  
79 water cycle. These include humidity, precipitation, P-E, and salinity. We also give  
80 recommendations that will lead towards more robust predictions and identification of  
81 the human influence on recent observed changes. It is beyond the scope of this paper to  
82 provide a full review of water cycle changes, or to discuss regional changes (see Parker  
83 2013; Collins et al. 2013b), changes in the biosphere and cryosphere, river discharge  
84 (see Dai et al. 2009), or drought (see Dai 2011a, 2011b, 2013; Trenberth et al. 2014).

85 We briefly describe the expected physical changes, before discussing the challenges of  
86 observing such changes with present observational capabilities, globally, as well as over  
87 ocean and land separately. We also discuss how physically consistent a picture these  
88 observations draw, and conclude with recommendations to ensure continued and  
89 improved ability to document the changing water cycle. The supplement provides more  
90 information on available observational data and quality control procedures.

91

## 92 **2. Expected changes in the global water cycle**

93 Changes in the hydrological cycle are an expected consequence of anthropogenic  
94 climate change. The Clausius-Clapeyron relationship suggests a strong quasi-  
95 exponential increase in water vapor concentrations with warming at about 6-7%/K  
96 near the surface. This is consistent with observations of change over the ocean (e.g.,  
97 Trenberth et al. 2005; Dai 2006a; Chung et al., 2014) and land (Dai 2006b; Willett et al.  
98 2010), and with simulations of future changes (e.g., Allen and Ingram 2002) and

99 assumes that on large scales the relative humidity changes little, as generally expected  
100 (see Sherwood et al. 2010; Allen and Ingram, 2002) and approximately seen in models  
101 (Richter and Xie 2008; Collins et al. 2013a). Locally, however, relative humidity changes  
102 may arise where large-scale circulation patterns alter, or when moisture sources are  
103 limited over land (e.g., Dai 2006; Vicente-Serrano et al. 2013).

104 *Changes in global mean precipitation* are limited by the energy budget, both through  
105 evaporation and the ability of the atmosphere to radiate away the latent heat released  
106 when precipitation forms (e.g., Trenberth 2011; O’Gorman et al. 2012). This largely  
107 explains why global mean precipitation increases by only 2-3% per K of warming in  
108 climate models (the ‘hydrological sensitivity’; see Figure 1). Broadly, the radiative effect  
109 of greenhouse gas forcing reduces the global precipitation increase driven by warming  
110 itself (e.g., Bony et al., 2013), while the direct radiative effect of aerosols that scatter  
111 rather than absorb sunlight does not influence the rate at which precipitation increases  
112 with warming. Figure 1 illustrates this for climate models run under the Coupled Model  
113 Intercomparison Project 5 (CMIP5) protocol (Taylor et al. 2012) for the 20<sup>th</sup> century,  
114 and for 4 standard scenarios for the 21st century. These range from RCP8.5, a high-  
115 emissions scenario, to RCP2.6, a low-emissions scenario (see Collins et al. 2013a). With  
116 stronger greenhouse gas forcing, global-mean temperature and precipitation both  
117 increase more, but the hydrological sensitivity becomes slightly smaller (see also Wu et  
118 al. 2010; Johns et al. 2011). Pendergrass and Hartmann (2014) show that the spread in  
119 CMIP5 model response of precipitation to increases in carbon dioxide is related to  
120 differences in atmospheric radiative cooling, which are in turn related to changes in  
121 temperature profiles and water vapor amounts. Forced changes in global-mean



122 precipitation are expected to be relatively small at present (Fig. 1b) and are therefore  
123 hard to distinguish from natural variability.

124 *Spatial patterns* are important both for identifying fingerprints of forced changes in  
125 precipitation and for impacts. Since global-mean evaporation and precipitation are  
126 expected to increase more slowly with temperature than implied by water vapor  
127 content, this implies slightly increased water vapor residence times and reduced  
128 atmospheric mass convergence (Vecchi et al. 2006; Held and Soden 2006). However,  
129 increasing water vapor more than offsets the weakened atmospheric wind convergence  
130 in the tropics (Vecchi et al. 2006; Held and Soden 2006; Allan 2012; Kitoh et al. 2013).  
131 Thus, where E exceeds P in the mean (such as over the sub-tropical oceans), it would do  
132 so even more, while areas where P exceeds E (such as the Intertropical Convergence  
133 Zone, ITCZ, and high latitudes) would receive yet more precipitation excess (Manabe  
134 and Wetherald 1980; Held and Soden 2006; Seager and Naik 2012; Bengtsson et al.  
135 2011, Bintanja and Selton, 2014). Simulations of future climate changes broadly confirm  
136 this, particularly when zonally averaged (see Fig. 2, bottom panel) and show rainfall  
137 generally increasing at latitudes and seasons that currently have high rainfall and less in  
138 dry regions (Collins et al. 2013a). This ‘wet get wetter, dry get drier’ paradigm involves  
139 a range of atmospheric processes, including an increased vertical gradient of  
140 atmospheric water vapor, which leads to intensified convective events in the deep  
141 tropics (see Chou et al. 2009).

142 However, simple P-E enhancement does not necessarily apply to dry land, where  
143 moisture is limited (Greve et al. 2014). It also does not hold true at regional scales,  
144 where atmospheric circulation changes may displace the geographical positions of

145 "wet" and "dry" regions (Xie et al., 2010; Chadwick et al., 2013; Allan 2014). GCMs  
146 generally simulate an expansion of the Hadley Cells as the globe warms, with associated  
147 poleward migration of subtropical aridity and storm tracks, but the size varies, and  
148 there is limited agreement on the mechanisms (Yin 2005; Lu et al. 2007; Seidel et al.  
149 2008; Scheff and Frierson 2012a, 2012b).

150 *Anthropogenic aerosol effects* counteract some of the anticipated greenhouse-gas driven  
151 warming, and hence the associated increase in precipitation (Liepert et al., 2004; Wu et  
152 al., 2013). Aerosols reduce the available energy for evaporation, and absorbing aerosols  
153 such as black carbon locally heat the atmosphere, effectively short-circuiting the  
154 hydrological cycle. Pendergrass and Hartmann (2012) show how black carbon forcing  
155 influences the inter-model spread in global-mean precipitation change in CMIP3  
156 models. The aerosol indirect effect may account for almost all aerosol cooling in models  
157 (Zelinka et al. 2014), and so be key to the aerosol-driven decrease in precipitation  
158 (Liepert et al., 2004; Levy et al 2013), although this is model-dependent (e.g., Shindell et  
159 al., 2012). The radiative effect of anthropogenic aerosols is also expected to affect the  
160 spatial pattern of precipitation and evaporation changes. As surface emissions of  
161 aerosol are spatially heterogeneous, and atmospheric residence times are relatively  
162 short, the direct radiative impact of aerosol is geographically variable, with the largest  
163 concentrations in the Northern Hemisphere (NH). The geographical heterogeneity of  
164 aerosol distribution is expected to affect the interhemispheric temperature gradient,  
165 and hence the atmospheric circulation – which should shift the ITCZ (e.g., Rotstayn et al.  
166 2000; Ming and Ramaswamy 2011; Hwang et al. 2013) and change the width of the  
167 Hadley cell (Allen et al. 2012). Models' representation of aerosols, and their  
168 interactions with clouds in particular, affect their ability to reproduce trends in the

169 interhemispheric temperature gradient (e.g. Chang et al., 2011; Wilcox et al. 2013).  
170 Modeling studies also suggest that aerosols may have contributed to the drying of the  
171 Sahel from 1940 to 1980 (Rotstayn and Lohmann, 2002; Ackerley et al. 2011; Hwang et  
172 al. 2013; Dong et al. 2014), and influence the East Asian monsoon (e.g. Lau et al. 2006;  
173 Meehl et al. 2008; Bollasina et al. 2011; Guo et al. 2012), and mid-latitude precipitation  
174 (Leibensperger et al. 2012; Rotstayn et al. 2012).

175 Stratospheric aerosols from explosive volcanic eruptions also influence the water cycle.  
176 Sharp reductions in observed global-mean land precipitation and stream flow were  
177 observed after the Mt Pinatubo eruption in 1991 (Trenberth and Dai 2007) and other  
178 20<sup>th</sup> century eruptions (Gu et al. 2007). This effect is particularly evident in  
179 climatologically wet regions, where the observed reduction in precipitation following  
180 eruptions appears significantly larger than simulated (Iles et al. 2014). Volcanoes may  
181 also contribute to regional drought by influencing the inter-hemispheric energy budget  
182 (e.g., Haywood et al. 2013).

183

### 184 **3. Observing and attributing changes in the global-scale water cycle**

185 Increases in atmospheric moisture are a key fingerprint of climate change. *Surface*  
186 *specific humidity* at global scales is reasonably well observed over land since 1973  
187 (HadISDH; Willett et al., 2013), and over ocean since 1971 (NOVSv2.0; Berry and Kent  
188 2009, 2011) using in situ data (for measurement techniques and more background as  
189 well as dataset information, see supplement); and results are quite robust across  
190 different data products (e.g., Dai 2006; Willett et al. 2007, 2013). Combined land and  
191 ocean surface specific humidity over the 1973-1999 period shows widespread

192 increases. This change has been attributed mainly to human influence (Willett et al.  
193 2007). As expected, globally, changes in *relative humidity* between 1973 and 1999 are  
194 small or negative (Hartmann et al., 2013). Since 2000, however, a decrease has been  
195 observed over land,- likely related to the greater warming of land relative to the ocean  
196 (Joshi et. al., 2008; Simmons et al., 2010; Willett et al., 2014).

197 In situ measurements of *atmospheric humidity* from radiosonde data provide time-  
198 series of Total Column Water Vapor (TCWV) from the 1950s. Increasing water vapor is  
199 apparent although spatial sampling is limited and temporal inhomogeneities are  
200 problematic (Dai et. al. 2011; Zhao et al. 2012). Global-scale patterns of change became  
201 observable only when the satellite era began. Since the 1980s, near-global satellite-  
202 based estimates of TCWV over the ice-free oceans and of clear-sky upper tropospheric  
203 relative humidity have allowed variability in tropospheric water vapor to be explored  
204 (e.g., Trenberth et al. 2005; Chung et al. 2014). The satellite-based Special Sensor  
205 Microwave Imager (SSM/I) TCWV data for 1988-2006 has enabled a robust  
206 anthropogenic fingerprint of increasing specific humidity to be detected over the oceans  
207 (Santer et al. 2007; 2009).

208 Satellite-based sensors, in combination with in situ data for best results, provide the  
209 only practical means for monitoring precipitation over land and ocean combined (e.g.,  
210 Fig 1). Satellite precipitation passive retrievals are restricted to the thermal infrared  
211 (IR) and microwave (MW) spectral bands. IR-based estimates are available from  
212 geostationary satellites at high frequency, but have modest skill at instantaneous  
213 rainfall intensity (e.g., Kidd and Huffman, 2011). Passive MW data, available since mid-  
214 1987, have made precipitation retrievals more reliable, and are particularly successful

215 over oceans. Retrievals over land are more approximate, since coasts and complex  
216 terrain increase uncertainty, and the accuracy of current algorithms deteriorates  
217 polewards of 50°. The latter is because these algorithms are tuned to lower-latitude  
218 conditions and because they cannot identify precipitation over snowy/icy surfaces.

219 Combined-satellite algorithms have been developed to merge individual estimates,  
220 either as relatively coarse-resolution, long-period climate data records (the Global  
221 Precipitation Climatology Project, GPCP, monthly dataset on a 2.5°x2.5°  
222 latitude/longitude grid begins in 1979; Adler et al. 2003), or, alternatively, as high-  
223 resolution precipitation products that start with the launch of the Tropical Rainfall  
224 Measuring Mission (TRMM) in late 1997 and will be continued with the successful  
225 launch of the Global Precipitation Mission (GPM) in early 2014. A recently released  
226 high-resolution dataset covers a somewhat longer period (Funk et al, 2014). Some  
227 products use rain-gauge data, where available, as input and to calibrate satellite-based  
228 rainfall estimates (Huffman et al. 2007). Therefore, satellite-derived products are not all  
229 independent of in situ data, and trends based on the satellite record may be affected by  
230 inhomogeneities in both the satellite and the surface data used (Maidment et al, 2014).

231 The satellite record has been very useful for understanding precipitation changes. A  
232 study sampling blended satellite observations of the wet and dry regimes as they shift  
233 spatially from year to year indicates enhanced seasonality (Chou et al. 2013), while Liu  
234 and Allan (2013) found tropical ocean precipitation increased by 1.7%/decade for the  
235 wettest 30% of the tropics in GPCP data, with declines over the remaining, drier, regions  
236 of -3.4%/decade for 1988-2008. Polson et al. (2013b) detected the fingerprint of a  
237 strengthening contrast of wet and dry regions in the GPCP satellite record since 1988,

238 and attributed this change largely to greenhouse gas increases. Marvel and Bonfils  
239 (2013) arrive at a similar conclusion, explicitly accounting for circulation changes and  
240 using the full record. Some of the changes detected in observations were significantly  
241 larger than modelled, for example, in wet regions over ocean (Polson et al. 2013b; see  
242 also Chou et al. 2013; Liu and Allan 2013).

243 *Atmospheric reanalyses* provide a global 3-dimensional and multi-decadal  
244 representation of changes in atmospheric circulation, fluxes and water vapor by  
245 assimilating observations (satellite, in situ, radiosondes, etc) into numerical weather  
246 prediction models. Notably, global quasi-observed P-E estimates are available only  
247 from reanalyses. Reanalyses, however, are affected by biases in the models and by long-  
248 term inhomogeneity of the observations, particularly, changing input data streams  
249 (Trenberth et al. 2005, 2011; Dee et al. 2011; Allan et al. 2014). These factors lead to  
250 inconsistencies between reanalyses and substantial uncertainties in their long-term  
251 trends; uncertainties that can be explored by using water budget closure constraints  
252 (e.g., Trenberth and Fasullo 2013a, b). The issues of long-term homogeneity will be  
253 improved in future developments (e.g. ERA-CLIM, <http://www.era-clim.eu>).

254 In conclusion, the satellite record is essential for monitoring the changing water cycle  
255 on a near-global scale, while future climate quality reanalyses hold considerable  
256 promise. Uncertainty estimates on long-term trends are difficult to provide (see  
257 supplement) but would be very useful.

258

#### 259 **4. Interpreting changes over ocean**

260 Changes in P-E and precipitation by climate models are particularly consistent over the  
261 oceans (Fig. 1b; Meehl et al. 2007; Bony et al. 2013). In terms of observations, in  
262 addition to the satellite record, limited in situ records are available, such as evaporation  
263 analyses (although fraught with discontinuities and global lack of closure) (Yu and  
264 Weller 2007; Yu et al. 2008) and precipitation from island stations and buoys (e.g., CRU,  
265 precipitation data as used in Josey and Marsh 2005). Overall, however, the in situ  
266 observations lack the spatial and temporal coverage needed to measure global changes  
267 (see Xie and Arkin 1998 for precipitation), and satellite and reanalysis data are  
268 consequently indispensable.

269 Both evaporation and precipitation affect local sea surface salinity. Thus, patterns and  
270 changes in the net freshwater flux, P-E, contribute to its temporal variations, and long-  
271 term changes to ocean salinity provide an important independent measurement from  
272 which the water cycle can be monitored. It should be noted, however, that in-situ ocean  
273 salinity is strongly influenced by changes to the ocean' circulation (which is influenced  
274 by ocean warming and surface wind changes), and thus that care must be taken when  
275 using in-situ salinity to infer P-E (Durack and Wijffels 2010; Skliris et al. 2014).

276 Ocean salinity observations have been made since the late 19<sup>th</sup> century by research  
277 cruises. Historical observational coverage is, however, sparse in the early part of the  
278 record, with near-global coverage achieved only recently (Supplementary Fig. 1), largely  
279 due to the Argo network of 3600 free-drifting floats initiated in 1999 (Freeland et al.  
280 2010). These floats measure the salinity and temperature of the upper 2000 m of the  
281 global ocean almost in real time. The Aquarius and Soil Moisture Ocean Salinity (SMOS)

282 satellite missions have provided global estimates of ocean surface salinity since late  
283 2009 and June 2011 respectively.

284 The observed pattern of salinity change at high latitudes and in the subtropics is  
285 broadly consistent with the expected changes in P-E, although the observational  
286 uncertainty is also clear (Fig. 3). These observed changes, broadly speaking, reflect an  
287 amplification of the climatological pattern of salinity – with salty regions getting saltier,  
288 and fresh regions getting fresher (Durack et al. 2012; Skliris et al. 2014). Observed  
289 salinity changes in the Atlantic and Pacific Ocean since the mid-20<sup>th</sup> century have been  
290 found to be outside the range of internal climate variability in model simulations, and  
291 have been attributed to anthropogenic influences (e.g. Stott et al. 2008; Terray et al.  
292 2012; Pierce et al. 2012). The attribution of salinity changes to anthropogenic factors  
293 was important evidence for the Intergovernmental Panel on Climate Change (IPCC)'s  
294 conclusion that there has been 'likely' a human contribution to the changing water cycle  
295 (see Bindoff et al., 2013). However, further work is required to better understand the  
296 effects of unforced variability on ocean salinity and their influence on the patterns of  
297 reported long-term changes,

298 It is essential that satellite-based, ship-based and Argo float measurements continue to  
299 monitor the ocean. Reliance on a single record type would hamper the identification of  
300 errors introduced by changes in coverage and measurement methods.

301

## 302 **5. Interpreting changes over land**

303 Over land, in situ data provide a long-term record of changing humidity and  
304 precipitation. However, the lack of reliable homogeneous terrestrial evapo-



305 transpiration data hampers studies of changes in the terrestrial water balance. Flux  
306 towers provide direct measurements of water, energy and carbon fluxes at a few points,  
307 but only for short periods (typically 5-15 years – e.g., Blyth et al. 2011). Pan evaporation  
308 can easily be diagnosed from general circulation climate models (GCMs; as “potential  
309 evaporation”) and effectively measures evaporative demand, which is very relevant to  
310 some crops and natural ecosystems. Long time-series would therefore be valuable (e.g.  
311 Greve et al. 2014), but measurements are sparse, and as it is not part of the actual  
312 energy or moisture budget it cannot be deduced from other measurements. Pan  
313 evaporation has decreased in many regions studied (related, at least partly, to wind  
314 stilling; McVicar et al. 2012), in contrast to actual evapotranspiration measured at  
315 Fluxnet sites, which increased until recently (Hartmann et al. 2013). Inferring  
316 evaporation from the atmospheric moisture budget in reanalyses (Trenberth et al.  
317 2011; Trenberth and Fasullo 2013b) is the most realistic option to analyse large-scale  
318 changes in P-E over land. As was mentioned above, however, reanalyses are affected by  
319 model error and their trends by changing data streams, and thus reanalysis evaporation  
320 data should be treated with caution.

321 The most widely used record of the changing water cycle over land is from long-term  
322 precipitation station data (e.g. Peterson and Vose 1997; Menne et al. 2012). Several  
323 gridded products are available (see Supplementary Table 1; Harris et al. 2014; Becker et  
324 al. 2013; Zhang et al. 2007), of which this paper shows three that have been processed  
325 differently, some completely interpolating precipitation over land (GPCC, Becker et al.,  
326 2013; CRU; Harris et al., 2014; with information on support available), or only providing  
327 values where long-term stations are available (Zhang et al., 2007). An additional dataset  
328 (VASCLIMO, Beck et al. 2005) uses a subset of GPCC stations that are considered long-

329 term and homogeneous. Figure 4 shows the density of the station network used in the  
330 CRU dataset, supplementary Fig. 2 for GPCC. Generally, data availability increased until  
331 1990, but has dropped since, especially in the tropics. For the GPCC this dramatic drop  
332 occurs a decade later. Country-specific readiness to share data is the biggest constraint  
333 for data density in the most recent decade.

334 The gridded precipitation datasets available vary also in their methods of quality  
335 control and homogenization (see Supplementary Material). This diversity leads to  
336 substantial differences in trends and discrepancies between datasets, and contributes to  
337 our uncertainty in how drought has changed (Trenberth et al. 2014).

338 Figure 5 illustrates similarities and differences in precipitation change from these  
339 datasets for high latitudes, and Figure 2, upper panel, for zonal mean changes. The  
340 zonal mean increase in northern high latitudes shown by most datasets (with the  
341 exception of the GPCC Full Data V6 dataset, which was not constructed with long-term  
342 homogeneity as a priority) agrees with expectation (see Fig. 2, lower panel), and is  
343 supported by Arctic regional studies (Rawlins et al. 2010). Min et al. (2008) detected the  
344 response to anthropogenic forcing in the observed moistening of northern high  
345 latitudes, using the Zhang et al. (2007) dataset. Figure 5, however, suggests substantial  
346 observational uncertainty, which may be partly due to coverage and data processing,  
347 and may contain a small contribution by changing liquid-to-solid ratio of precipitation  
348 (see discussion in supplement).

349 A substantial fraction of the differences between zonal changes recorded in different  
350 datasets can be explained by differences in spatial coverage (Polson et al. 2013a). The  
351 IPCC 5<sup>th</sup> Assessment report concluded that there is '*medium*' confidence in precipitation

352 change averaged over land after 1951 (and lower confidence before 1951) due to data  
353 uncertainty (Hartmann et al. 2013). Simulated changes in land precipitation are also  
354 uncertain, as evident from Fig. 1 (right panel).

355 The incomplete spatial coverage of precipitation changes in observations tends to  
356 increase noise and hence delay detection of global and large-scale changes (e.g., for  
357 precipitation changes, Balan Sarojini et al. 2012; Trenberth et al. 2014; note that in  
358 detection and attribution, only regions covered by observed data are analysed in both  
359 models and observations). Since station-based records are point measurements and  
360 precipitation tends to be highly variable spatially (e.g., Osborn, 1997), many stations are  
361 required to correctly reflect large-scale precipitation trends (e.g., Wan et al. 2013). In  
362 general, the variability in grid cells based on few stations is higher than if a larger  
363 number of stations are used, and changes may be recorded incompletely (see Zhang et  
364 al.,2007).

365 Despite these difficulties, zonal-mean precipitation changes agree better with the  
366 expected response to forcing than expected by chance, and show detectable changes for  
367 boreal winter and spring data (Polson et al. 2013a), as well as for annual data (see Fig. 2;  
368 Zhang et al. 2007; Polson et al. 2013a) for most datasets. These findings contributed to  
369 the IPCC 5<sup>th</sup> assessment's conclusion of 'medium confidence' that a human influence on  
370 global-scale land precipitation change is emerging (Bindoff et al. 2013). Wu et al. (2013)  
371 argue that the lack of an increase in Northern Hemispheric (NH) land precipitation over  
372 the last century is because aerosols induce a reduction in precipitation that counteracts  
373 the increase in precipitation expected from increases in greenhouse gases.

374 Due to data uncertainty, it is currently difficult to decide whether observed  
375 precipitation changes are larger than model simulated changes (Polson et al. 2013a).  
376 Averaging across mis-located precipitation features in models may reduce the  
377 magnitude of multi-model mean simulated precipitation change. This bias can be  
378 reduced by expressing changes relative to climatological precipitation (Noake et al.,  
379 2011; Liu and Allan, 2013; Polson et al. 2013b; Marvel and Bonfils, 2013), or by  
380 morphing model changes onto observed features (Levy et al. 2013a). However, in some  
381 cases, results still show observed changes that are large compared to model simulations  
382 (e.g., Polson et al. 2013a,b).

383 In summary, the record over land is extensive in time, but has serious limitations in  
384 spatial coverage and homogeneity. The drop in availability of recent in situ precipitation  
385 data (Fig. 4; supplementary Fig. 2) is of real concern. Data are particularly sparse in the  
386 tropics and subtropics, where substantial and spatially variable changes are expected.  
387 In addition to improving gauge density, more data-rescue funding and improved data-  
388 sharing practices and capabilities would help to address this problem.

389

## 390 **6. Intensification of precipitation extremes**

391 Since storms are fuelled by moisture convergence, storm-related extremes are expected  
392 to increase in a moister atmosphere (Emanuel 1999; Trenberth et al. 2003). It is less  
393 clear how large this increase will be, as limited moisture availability over land and  
394 possible stabilization of atmospheric temperature profiles tend to reduce the  
395 empirically derived response in precipitation extremes below the Clausius-Clapeyron-  
396 based increase in water vapor of 6-7%/K, while feedbacks of increased latent heat

397 release on storm intensity may amplify the response for sub-daily precipitation  
398 extremes (Lenderink and van Meijgaard 2008; Berg et al. 2013; Westra et al. 2014).  
399 Overall, under global warming, a substantial increase in the intensity of the stronger  
400 storms and precipitation events is expected. This increase is expected to be larger for  
401 more intense events (see Allen and Ingram 2002; Pall et al. 2011; Kharin et al. 2013;  
402 IPCC 2012), and is a robust fingerprint for the detection of climate change (Hegerl et al.  
403 2004).

404 This larger increase in intense precipitation than annual total precipitation implies light  
405 or no rain must become more common, suggesting longer dry spells and increased risk  
406 of drought, exacerbated by increased potential evapotranspiration (Trenberth et al.  
407 2003). How this intensification of extremes of the water cycle will be expressed is  
408 uncertain, as climate models still struggle to properly depict the diurnal cycle,  
409 frequency, intensity, and type of precipitation (see Flato et al. 2013), a problem which  
410 may be improved in part with the use of higher resolutions (e.g. Kendon et al. 2012;  
411 Strachan et al. 2013; Demory et al. 2014; Arakawa et al. 2011). Accurate representation  
412 of local storm dynamics may be an essential requirement for predicting changes to  
413 convective extremes (Kendon et al. 2014).

414 Worldwide in situ data for analysing changes in daily precipitation extremes have been  
415 collected by the CLIVAR Expert Team on Climate Change Detection and Indices (Donat  
416 et al. 2013). However, the record is far from complete in covering the global land  
417 masses, and is particularly sparse in key tropical regions. Increases in precipitation  
418 intensity have been identified in observations over many land regions (Fowler and  
419 Kilsby 2003; Groisman et al., 2005; Min et al. 2011; Zolina et al. 2010). Analysis of

420 observed annual maximum 1-day precipitation over land areas with sufficient data  
421 samples indicates an increase with global mean temperature of about 6-8%/K; Westra  
422 et al. 2013). Min et al. (2011) and Zhang et al. (2013) report detection of human  
423 influence on widespread intensification of extreme precipitation over NH land, although  
424 with substantial uncertainty in data and estimates of internal variability. Observed  
425 responses of daily precipitation extremes to interannual variability (e.g., Liu and Allan  
426 2012) potentially offer a constraint on climate change projections for future changes in  
427 extremes (O’Gorman 2012).

428 Characterizing sub-daily precipitation variability is difficult on large scales, given the  
429 limitations of the satellite record (see above), and agreement is poorer on short  
430 timescales than for multi-day averages (Liu and Allan 2012). However, a number of  
431 regional studies show recent increasing sub-daily precipitation intensities in response  
432 to rising temperatures (e.g., Lenderink and van Meijgaard 2008; Utsumi et al. 2011; see  
433 Westra et al., 2014). In the future, radar data exchanged globally show promise, if  
434 remaining technical and administrative problems can be resolved (e.g., Winterrath et al.  
435 2012a, 2012b; Michelson et al. 2013; Berg et al. 2013).

436 In short, it is essential to observe precipitation extremes to understand changing  
437 precipitation characteristics and quantify human-induced changes. However,  
438 uncertainties are substantial, and temporal and spatial scales reliably observable at  
439 present fall short of what is necessary for characterizing global changes.

440

## 441 **7. The challenge of climate variability**

442 Natural variability generated within the climate system can cause multi-decadal  
443 features in precipitation that are difficult to separate from the response to long-term  
444 forcing – especially in view of the relatively short observational record (e.g., Dai 2013).  
445 When determining if an observed change is significant relative to climate variability, a  
446 large sample of variability realizations from climate model simulations is generally  
447 used, since the observed record is short. However, discrepancies between simulated  
448 precipitation variability and that estimated from observations are substantial,  
449 particularly in the tropics (Zhang et al. 2007, see supplement) because of a combination  
450 of observational and model limitations. This introduces substantial uncertainty in  
451 detection and attribution results, even when model estimates of variance are doubled  
452 (as is often done; e.g., Zhang et al. 2007; Polson et al. 2013a). Long-term observed data  
453 obtained, for example, through data rescue are critical when evaluating simulations of  
454 multi-decadal variability ([www.oldweather.org](http://www.oldweather.org); [www.met-acre.org](http://www.met-acre.org), Allan et al. 2011).

455 Figure 6 illustrates how natural modes can induce apparent trends in precipitation over  
456 large regions (after Dai 2013). The Inter-decadal Pacific Oscillation index (IPO; closely  
457 related to the Pacific Decadal Oscillation, Liu 2012), for example, corresponds to an  
458 index of Southwest U.S. precipitation in observations and model experiments forced by  
459 sea surface temperatures (e.g. Schubert et al. 2009). This suggests that both an increase  
460 in Southwest U.S. precipitation from the late 1940s to early 1980s, and a subsequent  
461 decrease are largely caused by internal variability. El Niño and the IPO also influence  
462 precipitation patterns globally (Gu and Adler 2012; Dai 2013), which can influence  
463 trends over short periods such as those from satellites (Polson et al. 2013b; Liu and  
464 Allan 2013). This strong climate variability makes it difficult to detect the expected

465 long-term regional precipitation response to greenhouse gas forcing using historical  
466 data (see also Deser et al. 2012).

467 For understanding and attributing changes in the water cycle it is therefore important  
468 to account carefully for natural decadal climate variability, be it internally generated or  
469 volcanically forced. This is particularly true when using short records. Because un-  
470 forced internal variability is realization-dependent, discrepancies between model-based  
471 and observed records of variability should be expected and need to be accounted for in  
472 comparing models with observations for climatology, variability and trends.

473

## 474 **8. Conclusions and Recommendations**

475 There is strong evidence that changes are underway in aspects of the water cycle, which  
476 are consistent with theoretical expectations of the hydrological response to increased  
477 greenhouse gases and a warming planet. Many aspects of water cycle change, however,  
478 remain uncertain owing to small expected signals relative to the noise of natural  
479 variability, limitations of climate models, and short and inhomogeneous observational  
480 datasets.

481 Uncertainty may be reduced by cross-validating changes between multiple datasets and  
482 across variables, by putting these comparisons in the context of the theoretical  
483 expectation of the response of the water cycle to global climate change, and by exploring  
484 closure constraints. The observations, for example, suggest increases in high latitude  
485 precipitation, global-scale atmospheric humidity, and precipitation extremes that are  
486 consistent with expected changes. Furthermore, satellite data show signals of  
487 precipitation increases over wet regions and decreases over dry regions, corroborated



488 by in situ data over land, and physically consistent with an amplification of salinity  
489 patterns over the global ocean. The consistency in the evidence of changes of  
490 precipitation over land and from changes in ocean salinity is reflected in the IPCC's  
491 conclusion that human activity has 'likely' influenced the global water cycle since 1960  
492 (Bindoff et al. 2013), even though confidence in individual lines of evidence, such as  
493 attribution of precipitation changes to causes, is lower.

494 Observational uncertainty and a low signal-to-noise ratio pose serious difficulties when  
495 determining the magnitude of the human contribution to observed changes. Several  
496 studies report observed changes that are significantly larger than those simulated by  
497 climate models. However, these findings were generally not robust to data uncertainty.  
498 The uncertainty arises because the satellite record is short compared to decadal climate  
499 variability, and affected by calibration uncertainty; and because the available in situ  
500 record has many gaps, particularly in the tropics and subtropics, and is sparse on sub-  
501 daily timescales. Thus while observations can place constraints on future temperature  
502 changes, this is not yet possible for future precipitation projections (see Collins et al.  
503 2013 and Bindoff et al. 2013).

504 To improve the situation, we recommend:

505 1) *The satellite record is vital*, particularly to capture the strong changes over ocean  
506 that are robustly predicted by models. Only the full constellation can capture the  
507 intermittent nature of precipitation and capture extremes. The new GPM mission  
508 has exciting prospects for better calibration of space-based observations. Improved  
509 sampling by the constellation should enable the intermittency of precipitation to be  
510 better handled. Planning for future missions, providing continuity and temporal

511 overlap of measurements is essential to be able to reliably determine long-term  
512 trends.

513 2) *In situ stations* are vital both for cross-validating and calibrating satellite datasets  
514 and for long-term monitoring. However, the drop in available in situ data in recent  
515 decades, as illustrated for precipitation (Fig. 4), is alarming and needs to be  
516 addressed. Many observations are not made available for analysis, while some  
517 remain in paper form only and are not catalogued. It is necessary to strengthen  
518 efforts to rescue, scan and digitize data. Also, impediments to data sharing need to  
519 be overcome, and data delivery needs to be more timely in order to monitor the  
520 changing water cycle in near-real time, as is done for temperature.

521 3) There is need for better global coverage and higher time resolution data to capture  
522 *changing precipitation extremes*. Hourly datasets are needed to track and identify  
523 changes in short-term extremes, which are another important fingerprint of  
524 anthropogenic changes, and critical for flood management.

525 4) *Gridded products* of in situ precipitation change show substantial differences (Figs. 2,  
526 5), related to numbers of stations used, their homogeneity, manner of analysis,  
527 quality control procedures and treatment of changing data coverage over time. This  
528 uncertainty needs to be better characterized and best practices developed.

529 5) *Observations* in key regions are still sparse, particularly in the tropics, where the  
530 observing system is insufficient to record the anticipated changes in the water cycle.  
531 For the Asian monsoon, data sparsity is partly related to practical and  
532 administrative issues with data sharing. An improved international capacity to  
533 monitor all aspects of observed changes is important.

- 534 6) *Ocean salinity* observations provide an independent insight into the changing water  
535 cycle. Continued maintenance and improved coverage of the Argo Program, along  
536 with the development of satellite missions to follow Aquarius/SMOS for ocean  
537 salinity will strongly improve our understanding of global water cycle changes.
- 538 7) *Key diagnostics*, such as P-E, are not directly observable on large scales. Therefore,  
539 reanalysis data are vital, and their homogeneity in time and reliability for study of  
540 long-term changes need to be improved. Climate quality reanalysis will be very  
541 useful and are strongly encouraged. Closure of the water cycle using multiple  
542 variables provides a physical constraint that should be exploited to help quantify  
543 uncertainties.
- 544 8) Analyses of observed changes are more powerful if they make use of and diagnose  
545 *physical mechanisms* which are responsible for the atmospheric and oceanic change  
546 patterns. Studies need to investigate the robustness of results across data products,  
547 and evaluate the physical consistency of recorded changes across water cycle  
548 variables. Process studies may be able to constrain and better understand the fast  
549 circulation response to CO<sub>2</sub> forcing, which is a source of uncertainty.
- 550 9) *Uncertainty in the role of aerosols on precipitation is central when quantifying the*  
551 *human contribution to observed changes.* Aerosols vary enormously in space and  
552 time and in composition. Covariability with water vapor and clouds remain issues.  
553 Interactions between aerosol and cloud microphysics need to be better understood  
554 and represented in models, and the role of aerosol on precipitation changes needs to  
555 be better understood. This requires scientists from aerosol and water cycle  
556 communities to work together.

557 10) *Variability* generated within the climate system, particularly regionally on  
558 interannual to multidecadal timescales, has a large effect on water cycle variables  
559 and delays detection and emergence of changes. There is substantial uncertainty in  
560 present understanding about the magnitude and structure of variability in the water  
561 cycle which, if addressed, will improve the reliability of detection and attribution  
562 studies, and help societies in managing the impacts of decadal variability and  
563 change.

564

565

566 **Acknowledgements:**

567 We thank several anonymous reviewers for their helpful and perceptive suggestions.

568 The workshop that formed the basis for this paper was funded by NERC (the UK Natural  
569 Environment Research Council (NERC grant NE/I006672/1). We thank Eleanor Blyth  
570 and David Parker for comments. Robin Chadwick, Kate Willett, William Ingram, Lizzie  
571 Kendon and Peter Stott were supported by the Joint DECC/Defra Met Office Hadley  
572 Centre Climate Programme (GA01101). Paul Durack is supported by the Lawrence  
573 Livermore National Laboratory which is funded by the U.S. Department of Energy under  
574 contract DE-AC52-07NA27344, and William Ingram is partly supported by NERC grant  
575 NE/I00680X/1. Gabi Hegerl and Richard Allan are partly supported by NCAS. Kevin  
576 Trenberth is supported by NASA grant NNX11AG69G. NCAR is sponsored by The  
577 National Science Foundation. P.L. Vidale, R.P. Allan, B. Balan Sarojini, C. Liu, E. Black, P.  
578 Stott, G. Hegerl, D. Polson, R. Marsh, N. Skliris and Laura Wilcox are supported by the  
579 PAGODA project of the Changing Water Cycle programme of the UK Natural

580 Environment Research Council (NERC) under grant NE/I006672/1. A. Dai  
581 acknowledges the support of NSF grant #AGS-1353740. H.J. Fowler is supported by the  
582 CONVEX project of the Changing Water Cycle Programme of NERC under grant  
583 NE/I006680/1) and European Research Council funded INTENSE (ERC-2013-CoG).

584 **References**

- 585 Ackerley, D., B. B. Booth, S. H. E. Knight, E. J. Highwood, D. J. Frame, M. R. Allen, and D.  
586 P. Rowell, 2011: Sensitivity of Twentieth-Century Sahel Rainfall to Sulfate Aerosol and  
587 CO<sub>2</sub> Forcing. *J. Climate*, **24**, 4999–5014.
- 588 Adler, R. F., et al, 2003: The Version 2 Global Precipitation Climatology Project (GPCP)  
589 Monthly Precipitation Analysis (1979-Present). *J. Hydrometeor.*, **4**(6), 1147-1167.
- 590 Allan, R., P. Brohan, G. P. Compo, R. Stone, J. Luterbacher, and S. Brönnimann, 2011: The  
591 International Atmospheric Circulation Reconstructions over the Earth (ACRE) initiative.  
592 *Bull. Amer. Meteor. Soc.*, **92**, 1421-1425.
- 593 Allan, R. P., 2012: Regime dependent changes in global precipitation. *Clim. Dyn.*, **39**,  
594 doi:827-840 10.1007/s00382-011-1134-x.
- 595 Allan, R. P., 2014: Dichotomy of drought and deluge, *Nature Geosciences*,  
596 doi:10.1038/ngeo2243.
- 597 Allan, R. P., C., Liu, M. Zahn, D. A. Lavers, E. Koukouvagias, and A. Bodas-Salcedo, 2014:  
598 Physically consistent responses of the global atmospheric hydrological cycle in models  
599 and observations. *Surv. Geophysics.*, **35**, 533-552, doi: 10.1007/s10712-012-9213-z.
- 600 Allen, M. R., and W. J. Ingram, 2002: Constraints on future changes in climate and the  
601 hydrologic cycle. *Nature*, **419**, 224-232.
- 602 Allen, R. J., S. C. Sherwood, J. R. Norris and C. S. Zender, 2012: Recent Northern  
603 Hemisphere tropical expansion primarily driven by black carbon and tropospheric  
604 ozone, *Nature*, **485**, 350-355, doi:10.1038/nature11097

605 Andrews T., P. M. Forster, O. Boucher, N. Bellouin, and A. Jones, 2010: Precipitation,  
606 radiative forcing and global temperature change. *Geophys. Res. Lett.*, **37**, L14701,  
607 doi:10.1029/2010GL043991.

608 Arakawa, A., and J.-H. Jung, 2011: Multiscale Modeling of the Moist Convective  
609 Atmosphere A Review. *Atmos. Res.*, **102**, 263-285. doi:10.1016/j.atmosres.2011.08.009.

610 Arnell, N. W., and coauthors, 2013: A global assessment of the effects of climate policy  
611 on the impacts of climate change. *Nature Climate Change*, **3**, 512-519,  
612 doi:10.1038/nclimate1793

613 Balan Sarojini, B., P. A. Stott, E. Black, and D. Polson, 2012: Fingerprints of changes in  
614 annual and seasonal precipitation from CMIP5 models over land and ocean. *Geophys. Res.*  
615 *Letts.*, **39**, L21706, doi:10.1029/2012GL053373.

616 Beck, C., J. Grieser, and B. Rudolf, 2005: A New Monthly Precipitation Climatology for the  
617 Global Land Areas for the Period 1951 to 2000, *Climate status report*, 2004, 181–190,  
618 [http://www.dwd.de/bvbw/generator/DWDWWW/Content/Oeffentlichkeit/KU/KU4/  
619 KU42/en/VASClim0/pdf\\_28\\_precipitation,templateId=raw,property=publicationFile.  
620 pdf/pdf\\_28\\_precipitation.pdf](http://www.dwd.de/bvbw/generator/DWDWWW/Content/Oeffentlichkeit/KU/KU4/KU42/en/VASClim0/pdf_28_precipitation,templateId=raw,property=publicationFile.pdf/pdf_28_precipitation.pdf) (last access: 3 March 2013).

621 Becker, A., P. Finger, A. Meyer-Christoffer, B. Rudolf, K. Schamm, U. Schneider and M.  
622 Ziese, 2013: A description of the global land-surface precipitation data products of the  
623 Global Precipitation Climatology Centre with sample applications including centennial  
624 (trend) analysis from 1901-present. *Earth Syst. Sci. Data Discuss.*, **5**, 971-998.  
625 doi:10.5194/essd-5-71-2013

626 Bengtsson, L., K. I. Hodges, S. Koumoutsaris, M. Zahn, and N. Keenlyside 2011: The  
627 changing atmospheric water cycle in Polar Regions in a warmer climate. *Tellus*, **63A**,  
628 907–920.

629 Berg, P., C. Moseley, J. O. Haerter, 2013: Strong increase in convective precipitation  
630 response to higher temperatures, *Nature Geosci.*, **6**, doi:10.1038/NCEO1731.

631 Berry, D. I. and E. C. Kent, 2009: A new air-sea interaction gridded dataset from ICOADS  
632 with uncertainty estimates. *Bull. Am. Met. Soc.*, **90**, 645-656.

633 Berry, D. I. and E. C. Kent, 2011: Air-Sea fluxes from ICOADS: the construction of a new  
634 gridded dataset with uncertainty estimates. *Int. J. Climatol.*, **31**, 987-1001.

635 Bindoff, N., and coauthors, 2013: Detection and Attribution: from global to regional.  
636 Chapter 10: *Climate Change, 2013*. Contribution of Working Group 1 to the Fifth  
637 Assessment report of the Intergovernmental Panel on Climate Change [Stocker T. et al.  
638 (eds.)], Cambridge University Press, Cambridge UK and New York, NY, USA. 867-952.

639 Bintanja R and F. Selten, 2014: Future increases in Arctic precipitation linked to local  
640 evaporation and sea-ice retreat. *Nature* **509**, 479-482.

641 Blyth, E.M., D. B. Clark, R. Ellis, C. Huntingford, S. Los, M. Pryor, M. Best and S. Sitch,  
642 2011. A comprehensive set of benchmark tests for a land surface model of simultaneous  
643 fluxes of water and carbon at both the global and seasonal scale. *Geosci. Model Dev.*, **3**,  
644 1829–1859.

645 Bollasina M.A., Y. Ming, and V. Ramaswamy, 2011: Anthropogenic Aerosols and the  
646 Weakening of the South Asian Summer Monsoon. *Science*, **334**, 6055, 502-505.



647 Bony B. G. Bellon, D. Klocke, S. Sherwood, S. Fermepin, and S. Denvil, 2013 Robust direct  
648 effect of carbon dioxide on tropical circulation and regional precipitation. *Nature*  
649 *Geosci.*, **6**, 447–451.

650 Cao, L., G. Bala, and K. Caldeira, 2012: Climate response to changes in atmospheric  
651 carbon dioxide and solar irradiance on the time-scale of days to weeks. *Environ. Res.*  
652 *Lett.*, **7**, 034015, doi:10.1088/1748-9326/7/3/034015.

653 Chadwick, R. S., I. A. Boutle, and G. Martin, 2013: Spatial Patterns of Precipitation  
654 Change in CMIP5: Why the Rich do not get Richer in the Tropics. *J. Climate*, **26**, 3803-  
655 3822

656 Chang, C. Y., Chiang, J. C. H., Wehner, M. F., Friedman, A. R., & Ruedy, R. (2011). Sulfate  
657 Aerosol Control of Tropical Atlantic Climate over the Twentieth Century. *J. Climate*, **24**,  
658 2540-2555.

659 Chou, C., J. D. Neelin, C. A. Chen, and J. Y. Tu, 2009: Evaluating the "rich-get-richer"  
660 mechanism in tropical precipitation change under global warming. *J. Climate*, **22**, 1982-2005.

661 Chou C., J C H Chiang, C-W Lan, C-H Chung, Y-C Liao, C-J Lee, 2013: Increase in the range  
662 between wet and dry season precipitation, *Nature Geosci.*, doi:10.1038/ngeo1744.

663 Chung, E.-S., B. Soden, B. J. Sohn, and L. Shi, 2014: Upper-tropospheric moistening in  
664 response to anthropogenic warming, *PNAS*, **111**, 11636-11641,  
665 doi:10.1073/pnas.1409659111

666 Collins, M., and coauthors, 2013a: Long-term climate change: projections, commitments  
667 and irreversibility. Chapter 12: *Climate Change, 2013*. Contribution of Working Group 1  
668 to the Fifth Assessment report of the Intergovernmental Panel on Climate Change

669 [Stocker T. et al. (eds.)], Cambridge University Press, Cambridge, UK and New York, NY,  
670 USA. 1029-1136.

671 Collins M., K. Achuta-Rao, K. Ashok, S. Bhandari, A. K Mitra, S. Prakash, R. Srivastava and  
672 A. Turner, 2013b: Observational challenges in evaluating climate models. *Nature*  
673 *Climate Change*, **3**, 940-941.

674 Dai, A., 2006a: Recent climatology, variability and trends in global surface humidity. *J.*  
675 *Climate*, **19**, 3589-3606.

676 Dai A., 2006b: Precipitation characteristics in eighteen coupled climate models, *J.*  
677 *Climate*, **19**, 4605–4630.

678 Dai, A., 2011a: Drought under global warming: A review. *Wiley Interdisciplinary Reviews:*  
679 *Climate Change*, **2**, 45-65. DOI: 10.1002/wcc.81.

680 Dai, A., 2011b: Characteristics and trends in various forms of the Palmer Drought  
681 Severity Index during 1900–2008. *J. Geophys. Res.*, **116**, doi:10.1029/2010JD015541.

682 Dai, A., 2013a: Increasing drought under global warming in observations and models. *Nature*  
683 *Climate Change*. **3**: 52-58. doi:10.1038/nclimate1633.

684 Dai, A., 2013b: The influence of the Inter-decadal Pacific Oscillation on U.S. precipitation  
685 during 1923-2010. *Climate Dynamics*, **41**: 633-646. doi:10.1007/s00382-012-1446-5

686 Dai, A., T. Qian, K. E. Trenberth, and J. D Milliman, 2009: Changes in continental  
687 freshwater discharge from 1948-2004. *J. Climate*, **22**, 2773-2791.

688 Dee, D. P., and coauthors, 2011: The ERA-Interim reanalysis: configuration and  
689 performance of the data assimilation system. *Q.J.R. Meteorol. Soc.*, **137**, 553–597.  
690 doi:10.1007/s00382-013-1924-4

691 Demory, M.-E., P. L. Vidale, M. J. Roberts, P. Berrisford, J. Strachan, R. Schiemann, and M.  
692 S. Mizieliński, 2014: The role of horizontal resolution in simulating drivers of the global  
693 hydrological cycle. *Clim. Dyn.*, **42**, 2201-2225, doi:10.1007/s00382-013-1924-4.

694 Deser, C., A. S. Phillips, V. Bourdette, and H. Teng, 2012: Uncertainty in climate change  
695 projections: The role of internal variability. *Clim. Dyn.*, **38**, 527-546.

696 Dirmeyer, P. A., and coauthors, 2012: Simulating the diurnal cycle of rainfall in global  
697 climate models: resolution versus parameterization. *Clim. Dyn.*, **39**, 1-2, 399-418.

698 Donat, M. G., et al., 2013: Updated analyses of temperature and precipitation extreme  
699 indices since the beginning of the twentieth century: The HadEX2 dataset. *J. Geophys.*  
700 *Res. - Atmospheres*, **118**, 2098-2118. <http://dx.doi.org/10.1002/jgrd.50150>

701 Dong, B., Sutton, R. T., Highwood, E. J., and Wilcox, L. J., 2014: The Impacts of European  
702 and Asian Anthropogenic Sulfur Dioxide Emissions on Sahel Rainfall. *J. Climate*, **27**, 7000–  
703 7017, doi: <http://dx.doi.org/10.1175/JCLI-D-13-00769.1>

704 Durack, P. J. and S. E. Wijffels, 2010: Fifty-Year Trends in Global ocean salinities and  
705 their relationship to broad-scale warming. *J. Climate*, **23**, 4342-4362, doi:  
706 10.1175/2010JCLI3377.1

707 Durack, P. J., S. E. Wijffels and R. J. Matear, 2012: Ocean Salinities Reveal Strong Global  
708 Water Cycle Intensification During 1950–2000. *Science*, **336**, 455-458, doi:  
709 10.1126/science.1212222

710 Durack, P. J., S. E. Wijffels and T. P. Boyer (2013) Long-term Salinity Changes and  
711 Implications for the Global Water Cycle (Chapter 28). In: *Ocean Circulation and Climate*  
712 *(2<sup>nd</sup> Edition). A 21<sup>st</sup> century perspective* (Siedler, G., S.M. Griffies, J. Gould and J.A. Church

713 (Eds.)). International Geophysics, Academic Press, Elsevier, Oxford OX5 1GB, UK. **103**,  
714 727-757, doi: 10.1016/B978-0-12-391851-2.00028-3

715 Emanuel, K. A., 1999: Thermodynamic control of hurricane intensity. *Nature*, **401**, 665-  
716 669.

717 Flato, G., and coauthors, 2013: Evaluation of Climate Models. In: *Climate Change, 2013*.  
718 Contribution of Working Group 1 to the Fifth Assessment report of the  
719 Intergovernmental Panel on Climate Change [Stocker T. et al. (eds.)], Cambridge  
720 University Press, Cambridge, UK and New York, NY, USA.

721 Fowler, H. J., and C. G. Kilsby, 2003: Implications of changes in seasonal and annual  
722 extreme rainfall. *Geophys. Res. Lett.*, **30**, 1720, doi:10.1029/2003GL017327.

723 Freeland, H. & Co-Authors, 2010: Argo - A decade of progress. *Proceedings of*  
724 *OceanObs'09: Sustained Ocean Observations and Information for Society (Vol. 2)*, Venice,  
725 Italy, 21-25 September 2009, Hall, J., Harrison, D.E. & Stammer, D., Eds., ESA Publication  
726 WPP-306, doi:10.5270/OceanObs09.cwp.32.

727 Funk, C.C., P.J. Peterson, M. F. Landsfeld, D. H. Pedreros, J. P. Verdin, J. D. Rowland, B. E.  
728 Romero, G. J. Husak, J. C. Michaelsen, and A. P. Verdin, 2014: A quasi-global precipitation  
729 time series for drought monitoring: *U.S. Geological Survey Data Series* **832**, 4p.,  
730 <http://dx.doi.org/10.3133/ds832>

731 Gillett, N. P., A. J. Weaver, F. W. Zwiers, and M. F. Wehner, 2004:  
732 Detection of volcanic influence on global precipitation.  
733 *Geophys. Res. Lett.*, **31**, L12217, doi:10.1029/2004GL020044.

734 Gimeno, L., A. Stohl, R. M. Trigo, F. Dominguez, K. Yoshimura, L. Yu, A. Drumond, A. M.  
735 Durán-Quesada, and R. Nieto, 2012: Oceanic and Terrestrial Sources of Continental  
736 Precipitation, *Rev. Geophys.*, **50**, RG4003, doi:10.1029/2012RG000389.

737 Grabowski, W. W., 2001: Coupling cloud processes with the large-scale dynamics using  
738 the cloud-resolving convection parameterization (CRCP). *J. Atmos. Sci.*, **58**, 978–997.

739 Greve, P., B. Orlowsky, B. Mueller, J. Sheffield, M. Reichstein, and S. I. Seneviratne, 2014:  
740 Global assessment of trends in wetting and drying over land, *Nature Geoscience*.  
741 doi:10.1038/ngeo2247 (early online release)

742 Groisman, P. Y., R. W. Knight, D. R. Easterling, T. R. Karl, G. C. Hegerl, and V. N. Razuvaev,  
743 2005: Trends in intense precipitation in the climate record. *J. Climate*, **18**, 1326–1350.

744 Gu, G., R. F. Adler, G. J. Huffman, and S. Curtis, 2007: Tropical Rainfall Variability on  
745 Interannual-to-Interdecadal/Longer-Time Scales Derived from the GPCP Monthly  
746 Product. *J. Climate*, **20**, 4033-4046.

747 Gu, G., and R. F. Adler, 2012: Interdecadal Variability/Long-Term Changes in Global  
748 Precipitation Patterns during the Past Three Decades: Global Warming and/or Pacific  
749 Decadal Variability? *Clim. Dyn.*, **40**, 3009-3022. doi:10.1007/s00382-012-1443-8.

750 Guo, L., E. J. Highwood, L. C. Shaffrey, and A. G. Turner, 2012: The effect of regional  
751 changes in anthropogenic aerosols on rainfall of the East Asian Summer Monsoon.  
752 *Atmos. Chem. Phys. Discuss.*, **12**, 23007-23038.

753 Harris, I., Jones, P. D., Osborn, T. J. and Lister, D. H., 2014: Updated high-resolution grids  
754 of monthly climatic observations - the CRU TS 3.1 Dataset. *Int. J. Climatol.*, **34**, 623-642.  
755 doi:10.1002/joc.3711.

756 Hartmann, D., and coauthors, 2013: Observations: atmosphere and surface. Chapter 2,  
757 *Climate Change 2013; The physical science basis. Contribution of Working Group 1 to the*  
758 *Fifth Assessment report of the Intergovernmental Panel on Climate Change* [Stocker T. et  
759 al. (eds.)], Cambridge University Press, 159-254.

760 Haywood, J. M., A. Jones, N. Bellouin, and D. Stephenson, 2013: Asymmetric forcing from  
761 stratospheric aerosols impacts Sahelian rainfall. *Nature Climate Change*, **3**, 660–665.

762 Hegerl G. C., F. W. Zwiers, P. A. Stott, and V. V. Kharin, 2004: Detectability of  
763 anthropogenic changes in annual temperature and precipitation extremes. *J. Climate*,  
764 **17**, 3683-3700.

765 Hegerl, G. C. , and F. W. Zwiers, 2011: Use of models in detection and attribution of  
766 climate change. *WIREs Clim Change*, **2**, 570–591.

767 Held, I. M., and B. J. Soden, 2006: Robust responses of the hydrological cycle to global  
768 warming. *J. Climate*, **19**, 5686–5699.

769 Huffman, G.J., R. F. Adler, D. T. Bolvin, G. Gu, E. J. Nelkin, K. P. Bowman, Y. Hong, E. F.  
770 Stocker, D. B. Wolff, 2007: The TRMM Multi-satellite Precipitation Analysis: Quasi-  
771 Global, Multi-Year, Combined-Sensor Precipitation Estimates at Fine Scale. *J.*  
772 *Hydrometeor.*, **8**, 38-55.

773 Huffman, G. J., R. F. Adler, D. T. Bolvin, and G. Gu, 2009: Improving the global  
774 precipitation record: GPCP Version 2.1, *Geophys. Res. Lett.*, **36**, L17808,  
775 doi:10.1029/2009GL040

776 Hwang, Y.-T., D. M. W. Frierson, and S. M. Kang, 2013: Anthropogenic sulfate aerosol and  
777 the southward shift of tropical precipitation in the late 20th century, *Geophys. Res. Lett.*,  
778 **40**, 2845–2850.

779 Iles C. and G.C. Hegerl 2014: The global precipitation response to volcanic eruptions in the  
780 CMIP5 models. *Environmental Research Letters*, in press.

781 IPCC, 2012: Managing the Risks of Extreme Events and Disasters to Advance Climate  
782 Change Adaptation. *A Special Report of Working Groups I and II of the Intergovernmental*  
783 *Panel on Climate Change* [Field, C.B., et al. (eds.)]. Cambridge University Press,  
784 Cambridge, UK, and New York, NY, USA, 582 pp.

785 IPCC, 2013: Summary for Policymakers, In: Climate Change, 2013: *The Physical Science*  
786 *Basis*. Contribution of Working Group 1 to the IPCC Fifth Assessment Report Climate  
787 Change 2013 [Stocker, T. et al. (eds)]., Cambridge University Press, Cambridge, UK and  
788 New York, NY, USA..

789 Johns, T. J., and coauthors, 2011: Climate Change under aggressive mitigation: the  
790 ENSEMBLES multi-model experiment. *Clim. Dyn.*, **37**, 1975-2003.

791 Josey, S. A. and R. Marsh, 2005: Surface freshwater flux variability and recent freshening  
792 of the North Atlantic in the Eastern Subpolar Gyre, *J. Geophys. Res.*, **110**, C05008,  
793 doi:10.1029/2004JC002521.

794 Joshi, M. M., J. M. Gregory, M. J. Webb, D. M. Sexton and T. C. Johns, 2008: Mechanisms for  
795 the land/sea warming contrast exhibited by simulations of climate change. *Clim. Dyn.*,  
796 **30**, 5455-465.

797 Kendon, E. J., N. M. Roberts, C. A. Senior, and M. J. Roberts, 2012: Realism of Rainfall in a  
798 Very High-Resolution Regional Climate Model. *J. Climate*, **25**, 5791–5806.

799 Kendon, E. J., N. M. Roberts, H. J. Fowler, M. J. Roberts, S. C. Chan, and C. A. Senior, 2014:  
800 Heavier summer downpours with climate change revealed by weather forecast  
801 resolution model. *Nature Climate Change* **4**, 570–576, doi:10.1038/nclimate2258.

802 Kenyon, J., and G. C. Hegerl, 2010: Influence of modes of climate variability on global  
803 precipitation extremes. *J. Climate*, **23**, 6248–6262.

804 Kharin, V. V., F. W. Zwiers, X. Zhang, and G. C. Hegerl, 2007: Changes in temperature and  
805 precipitation extremes in the IPCC ensemble of global Coupled Model Simulations, *J.*  
806 *Climate*, **20**, 1419-1444.

807 Kharin, V. V., F.W. Zwiers, X. Zhang, and M. Wehner, 2013: Changes in temperature and  
808 precipitation extremes in the CMIP5 ensemble. *Climatic Change*, **19**, 345-359.  
809 doi:10.1007/s10584-013-0705-8.

810 Kidd, C., and G.J. Huffman, 2011: Global Precipitation Measurement. *Meteor. Appl.*, **18**(3),  
811 doi:10.1002/met.284, 334-353.

812 Kitoh, A., H. Endo, K. Krishna Kumar, I. F. A. Cavalcanti, P. Goswami, and T. Zhou, 2013:  
813 Monsoons in a changing world: A regional perspective in a global context, *J. Geophys. Res.*  
814 *Atmos.*, **118**, 3053–3065, doi:10.1002/jgrd.50258

815 Kundzewicz, Z. W., L. J. Mata, N. W. Arnell, P. Döll, P. Kabat, B. Jiménez, K. A. Miller, T. Oki,  
816 Z. Sen and I. A. Shiklomanov, 2007: Freshwater resources and their management.  
817 *Climate Change 2007: Impacts, Adaptation and Vulnerability. Contribution of Working*  
818 *Group II to the Fourth Assessment Report of the Intergovernmental Panel on Climate*



819 *Change*, M. L. Parry, O. F. Canziani, J. P. Palutikof, P. J. van der Linden and C. E. Hanson,  
820 Eds., Cambridge University Press, Cambridge, UK, 173-210.

821 Lambert H, M. Webb, 2008: Dependence of global mean precipitation on surface  
822 temperature. *Geophys. Res. Lett.* **35**, doi:10.1029/2008GL034838

823 Lau, K. M., M. K. Kim, and K. M. Kim, 2006: Asian summer monsoon anomalies induced  
824 by aerosol direct forcing: the role of the Tibetan Plateau. *Clim. Dyn.*, **26**, 855-864.

825 Lazo, J. K., M. Lawson, P. H. Larsen, and D. M. Waldman, 2011: U.S. Economic Sensitivity  
826 to Weather Variability. *Bull. Amer. Meteor. Soc.*, **92**, 709–720.

827 Leibensperger, E. M., L. J. Mickley, D. J. Jacob, W. -T. Chen, J. H. Seinfeld, A. Nenes, P. J.  
828 Adams, D. G. Streets, N. Kumar, D. Rind, 2012: Climatic effects of 1950-2050 changes in  
829 US anthropogenic aerosols - Part 2: Climate response, *Atmos. Chem. Phys.*, **12**(7), 3349-  
830 3362.

831 Lenderink, G., and E. van Meijgaard, 2008, Increase in hourly precipitation extremes  
832 beyond expectations from temperature changes. *Nature Geos.*, **1**, 511-514.

833 Levy, A. A., L. W. Ingram, M. Jenkinson, C. Huntingford, F. H. Lambert, and M. Allen,  
834 2013a: Can correcting feature location in simulated mean climate improve agreement  
835 on projected changes? *Geophys. Res. Lett.*, **40**, 354–358, doi:10.1029/2012GL053964.

836 Levy II, H., L. W. Horowitz, M. D. Schwarzkopf, Y. Ming, J.-C. Golaz, V. Naik, and V.,  
837 Ramaswamy, 2013b: The roles of aerosol direct and indirect effects in past and future  
838 climate change. *J. Geophys. Res.*, **118**, 4521–4532.

839 Liepert, B. G., J. Feichter, U. Lohmann and E. Roeckner, 2004: Can aerosols spin down the  
840 water cycle in a warmer and moister world?. *Geophys. Res. Lett.* 31(6), L06207.

841 Liepert, B. G., and and F. Lo, 2013: CMIP5 update of 'Inter-model variability and biases  
842 of the global water cycle in CMIP3 coupled climate models' *Environ. Res. Lett.* **8** 029401,  
843 doi:10.1088/1748-9326/8/2/029401.

844 Liu, C., and R. P. Allan, 2012: Multisatellite observed responses of precipitation and its  
845 extremes to interannual climate variability. *J. Geophys. Res.*, **117**, D03101,  
846 doi:10.1029/2011JD016568.

847 Liu, C. and R. P. Allan, 2013: Observed and simulated precipitation responses in wet and  
848 dry regions 1850-2100, *Environ. Res. Lett.*, **8**, 034002, doi:10.1088/1748-  
849 9326/8/3/034002

850 Liu, Z. Y., 2012: Dynamics of interdecadal climate variability: A historical perspective. *J.*  
851 *Climate*, **25**, 1963-1995.

852 Lu, J., G. Vecchi, and T. Reichler, 2007: Expansion of the Hadley cell under global warming.  
853 *Geophys. Res. Letts.*, **34**, L06805, doi:10.1029/2006GL028443.

854 Maidment, R., D Grimes, R.P. Allan, E. Tarnavsky, M. Stringer, T. Hewison, R. Roebeling  
855 and E. Black (2014) The 30 year TAMSAT African Rainfall Climatology And Time series  
856 (TARCAT) data set *Journal of Geophysical Research* doi: 10.1002/2014JD021927

857 Manabe, S., and R. T. Wetherald, 1980: On the distribution of climate change resulting  
858 from an increase in CO<sub>2</sub> content of the atmosphere. *J. Atmos. Sci.*, **37**, 99–118.

859 Marvel K, and C. Bonfils, 2013: Identifying external influences on global precipitation.  
860 *PNAS*, **110** (48) 19301-19306, doi: 10.1073/pnas.1314382110.

861 Meehl, G. A., and coauthors, 2007: Global Climate Projections. In: Climate Change 2007:  
862 The Physical Science Basis. Contribution of Working Group I to the Fourth Assessment

863 Report of the Intergovernmental Panel on Climate Change [Solomon, S., D. Qin, M.  
864 Manning, Z. Chen, M. Marquis, K.B. Averyt, M. Tignor and H.L. Miller (eds.)]. Cambridge  
865 University Press, Cambridge, United Kingdom and New York, NY, USA

866 Meehl, G. A., J. M. Arblaster, and W. D. Collins, 2008: Effects of black carbon aerosols on  
867 the Indian monsoon. *J. Climate*, **21**, 2869-2882.

868 Menne, M. J., I. Durre, R. S. Vose, B. E. Gleason, and T. G. Houston, 2012: An overview of  
869 the Global Historical Climatology Network daily database. *J. Atmos. Oceanic Technol.*, **29**,  
870 897–910.

871 Merrifield, M. A., 2011: A Shift in Western Tropical Pacific Sea Level Trends during the  
872 1990s. *J. Climate*, **24**, 4126–4138.

873 Michelson, D., and coauthors, 2013: WMO Initiative for the global exchange of radar  
874 data. *Proc. AMS Radar Conf.*

875 Min, S., X. Zhang, and F. W. Zwiers, 2008: Human-induced Arctic moistening. *Science*,  
876 **320**, 518-520.

877 Min, S, X. Zhang, F. F Zwiers, and G. C. Hegerl, 2011: Human contribution to more intense  
878 precipitation extremes. *Nature*, **470**, 378–381.

879 Ming, Yi, and V. Ramaswamy, 2011: A Model Investigation of Aerosol-Induced Changes  
880 in Tropical Circulation. *J. Climate*, **24**, 5125–5133.

881 Morice, C. P., J. J. J. Kennedy, N. A. Rayner, and P. D. Jones, 2012: Quantifying  
882 uncertainties in global and regional temperature change using an ensemble of  
883 observational estimates: The HadCRUT4 dataset, *J. Geophys. Res.*, **117**, D08101  
884 [doi:10.1029/2011JD017187](https://doi.org/10.1029/2011JD017187).

885 Noake, K., D. Polson, G. C. Hegerl, and X. Zhang, 2012, Changes in seasonal land  
886 precipitation during the latter twentieth-century. *Geophys. Res. Letts.*, **39**, L03706,  
887 doi:10.1029/2011GL050405.

888 O’Gorman, P. A., 2012: Sensitivity of tropical precipitation extremes to climate change.  
889 *Nature Geosci.*, **5**, 697–700.

890 O’Gorman, P. A., R. P. Allan, M. P. Byrne, and M. Previdi, 2012: Energetic constraints on  
891 precipitation under climate change. *Surv. Geophys.*, **33**, 585-608.

892 Osborn, T. J., 1997: Areal and point precipitation intensity changes: implications for the  
893 application of climate models. *Geophys. Res. Lett.*, **24**, 2829-2832  
894 doi:10.1029/97GL02976.

895 Pall, P and coauthors, 2011: Anthropogenic greenhouse gas contribution to UK autumn  
896 flood risk. *Nature*, **470**, 382–385.

897 Parker, D, 2013: Global precipitation datasets for climate monitoring, attribution and  
898 model assessment. Met Office Hadley Centre technical note, October, 2013.

899 Pendergrass, A. G., and D. L. Hartmann 2012: Global-mean precipitation and black carbon in  
900 AR4 simulations, *Geophys. Res. Lett.*, **39**, L01703, doi:10.1029/ 2011GL050067.

901 Pendergrass, A. and D. Hartmann, 2014: The atmospheric energy constraint on global-  
902 mean precipitation change. *J. Clim.*, **27**, 757-768, doi:10.1175/JCLI-D-13-00163.1.

903 Peterson, B. J., R. M. Holmes, J. W. McClelland, C. J. Vorosmarty, R. B. Lammers, A. I.  
904 Shiklomanov, I. A. Shiknomanov, and S. Rahmstorf, 2002: Increasing river discharge to  
905 the Arctic Ocean. *Science*, **298**, 2171–2173.

906 Peterson, T. C., and R. Vose, 1997: An overview of the global historical climatology  
907 network temperature database. *Bull. Amer. Meteor. Soc.*, **78**, 2837-2849.

908 Peterson, T. C., P. A. Stott, and S. Herring, 2012: Explaining Extreme Events of 2011 from  
909 a Climate Perspective. *Bull. Amer. Meteor. Soc.*, **93**, 1041–1067.

910 Peterson, T. C., M. P. Hoerling, P. A. Stott and S. Herring, Eds., 2013: Explaining Extreme  
911 Events of 2012 from a Climate Perspective. *Bull. Amer. Meteor. Soc.*, **94**(9), S1–S74.

912 Pierce, D. W., P. J. Gleckler, T. P. Barnett, B. D. Santer, and P. J. Durack, 2012: The  
913 fingerprint of human-induced changes in the ocean’s salinity and temperature fields.  
914 *Geophys. Res. Lett.*, **39**, L21704, doi: 10.1029/2012GL053389.

915 Polson, D., G. C. Hegerl, X. Zhang, and T. J. Osborn, 2013a: Causes of robust seasonal land  
916 precipitation changes. . *J. Climate*, **20**, 6679-6697. Polson, D., G. C. Hegerl, R. P. Allan, and  
917 B. Balan Sarojini, 2013b: Have greenhouse gases intensified the contrast between wet  
918 and dry regions? *Geophys. Res. Lett.*, **40**, 4783-4787, doi:10.1002/grl.50923.

919 Rawlins, Michael A., and Coauthors, 2010: Analysis of the Arctic System for Freshwater  
920 Cycle Intensification: Observations and Expectations. *J. Climate*, **23**, 5715–5737.

921 Richter, I., and S. P. Xie, 2008: Muted precipitation increase in global warming simulations:  
922 A surface evaporation perspective, *J Geophys Res-Atmos*, *113*, D24118, doi:  
923 24110.21029/22008JD010561.

924 Rotstayn, L. D., B. F. Ryan, and J. E. Penner, 2000: Precipitation changes in a GCM  
925 resulting from the indirect effects of anthropogenic aerosols, *Geophys. Res. Lett.*, **27**,  
926 3045-3048.

927 Rotstayn, L. D., and U. Lohmann, 2002: Tropical Rainfall Trends and the Indirect Aerosol  
928 Effect. *J. Climate*, **15**, 2103–2116.

929 Rotstayn, L.D., Jeffrey, S.J., Collier, M.A., Dravitzki, S.M., Hirst, A.C., Syktus, J.I., and K.K.  
930 Wong, 2012: Aerosol induced changes in summer rainfall and circulation in the  
931 Australasian region: a study using single-forcing climate simulations. *Atmos. Chem. Phys.*  
932 *Disc.*, **12**, 5107-5188.

933 Santer, B. D., and coauthors, 2007: Identification of human-induced changes in  
934 atmospheric moisture content. *Proc. Natl. Acad. Sci. USA*, **104**, 15244–15253.

935 Santer, B. D., and coauthors, 2009: Incorporating model quality information in climate  
936 change detection and attribution studies. *Proc. Natl. Acad. Sci. USA*, **106** 14778-14783.

937 Scheff, J., and D. Frierson, 2012a: Twenty-first-century multimodel subtropical  
938 precipitation declines are mostly midlatitude shifts. *J. Climate.*, **25**, 4330-4347.

939 Scheff, J., and D. Frierson, 2012b: Robust future precipitation declines in CMIP5 largely  
940 reflect the poleward expansion of model subtropical dry zones. *Geophys. Res. Lett.*, **39**,  
941 L18704, doi:10.1029/2012GL052910.

942 Schubert, S., and coauthors, 2009: A USCLIVAR project to assess and compare the  
943 responses of global climate models to drought-related SST forcing patterns: Overview  
944 and results. *J. Climate*, **22**, 5251-5272.

945 Seager, R., and N. Naik, 2012: A mechanisms-based approach to detecting recent  
946 anthropogenic hydroclimate change, *J. Climate*, **25**, 236–261.

947 Seidel, D. J., Q. Fu, W. J. Randel, and T. J. Reichler, 2008: Widening of the tropical belt in a  
948 changing climate. *Nature Geosci.*, **1**, 21–24.

949 Sherwood, S. C., R. Roca, T. M. Weckwerth, and N. G. Andronova, 2010: Tropospheric  
950 water vapour, convection and climate. *Rev. Geophysics*, **48**, RG2001,  
951 doi:10.1029/2009RG000301.

952 Shindell, D., Voulgarakis, A., Faluvegi, G., and Milly, G., 2012: Precipitation response to  
953 regional radiative forcing. *Atmos. Chem. Phys.* **12** 6969–6982.

954 Simmons, A. J., K. M. Willet, P. D Jones, P. W. Thorne, and D. P. Dee, 2010: Low frequency  
955 variations in surface atmospheric humidity, temperature, and precipitation: Inferences  
956 from reanalyses and monthly gridded observational data sets. *J. Geophys. Res.*, **115**,  
957 D01110, doi:10.1029/2009JD012442.

958 Skliris, N., Marsh, R., Josey, S. A., Good, S. A., Liu, C., and R. P. Allan, 2014: Salinity changes  
959 in the World Ocean since 1950 in relation to changing surface freshwater fluxes. *Clim.*  
960 *Dyn.*, doi:10.1007/s00382-014-2131-7

961 Stephens, G. L. and T. D. Ellis, 2008: Controls of global-mean precipitation increases in  
962 global warming GCM experiments. *J. Climate*, **21**, 6141-6155.

963 Stott, P. A., R. T. Sutton and D. M. Smith, 2008: Detection and attribution of Atlantic  
964 salinity changes. *Geophys. Res. Lett.*, **35**, L21702, doi:10.1029/2008GL035874.

965 Stott, P. A., N. P. Gillett, G. C. Hegerl, D. J. Karoly, D. A. Stone, X. Zhang, and F. Zwiers,  
966 2010: Detection and attribution of climate change: a regional perspective. *WIREs Clim*  
967 *Change*, **1**, 192-211. doi:10.1002/wcc.34

968 Strachan, J., P. L. Vidale, K. Hodges, M. Roberts, M.-E. Demory, 2013: Investigating Global  
969 Tropical Cyclone Activity with a Hierarchy of AGCMs: The Role of Model Resolution. *J.*  
970 *Climate*, **26**, 133–152.

971 Taylor, K.E, R. J. Stouffer, and G. A. Meehl, 2012: An Overview of CMIP5 and the  
972 Experiment Design. *Bull. Amer. Meteor. Soc.*, **93**, 485–498.

973 Terray, L., L. Corre, S. Cravatte, T. Delcroix, G. Reverdin, and A. Ribes, 2012: Near-Surface  
974 Salinity as Nature’s Rain Gauge to Detect Human Influence on the Tropical Water Cycle.  
975 *J. Climate*, **25**, 958–977.

976 Trenberth, K. E., 2011: Changes in precipitation with climate change. *Climate Research*,  
977 **47**, 123-138, doi:10.3354/cr00953.

978 Trenberth, K. E., A. Dai, R. M. Rasmussen and D. B. Parsons, 2003: The changing  
979 character of precipitation. *Bull. Amer. Meteor. Soc.*, **84**, 1205-1217.

980 Trenberth, K. E. , J. Fasullo J, and L. Smith, 2005: Trends and variability in column-  
981 integrated water vapor. *Clim. Dyn.*, **24**, 741–758.

982 Trenberth, K. E., and A. Dai, 2007: Effects of Mount Pinatubo volcanic eruption on the  
983 hydrological cycle as an analog of geoengineering. *Geophys. Res. Lett.*, **34**, L15702,  
984 doi:10.1029/2007GL030524.

985 Trenberth, K. E., J. T. Fasullo, and J. Mackaro, 2011: Atmospheric moisture transports  
986 from ocean to land and global energy flows in reanalyses. *J. Climate*, **24**, 4907-4924.

987 Trenberth, K. E., and J. T. Fasullo, 2013a: North American water and energy cycles.  
988 *Geophys. Res. Lett.*, **40**, 365–369, doi:10.1002/grl.50107.

989 Trenberth, K. E., and J. T. Fasullo, 2013b: Regional energy and water cycles: Transports  
990 from ocean to land. *J. Climate*, **26**, 7837-7851, doi:10.1175/JCLI-D-00008.1.



991 Trenberth, K. E., A. Dai, G. van der Schrier, P. D. Jones, J. Barichivich, K. R. Briffa, and J.  
992 Sheffield, 2014: Global warming and changes in drought. *Nature Climate Change*, **4**, 17-  
993 22, doi:10.1038/nclimate2067.

994 Vecchi, G. A., B. J. Soden, A. T. Wittenberg, I. M. Held, A. Leetmaa, and M. J. Harrison,  
995 2006: Weakening of tropical Pacific atmospheric circulation due to anthropogenic  
996 forcing. *Nature*, **441**, 73–76.

997 McVicar T. M. et al., 2012: Global review and synthesis of trends in observed terrestrial  
998 near-surface wind speeds: Implications for evaporation. *J. Hydrol.*, **416**, 182-205.

999 Vicente-Serrano, S. M., C. Azorin-Molina, A. Sanchez-Lorenzo, E. Morán-Tejeda, J.  
1000 Lorenzo-Lacruz, J. Revuelto, J. I. López-Moreno, and F. Espejo, 2013: Temporal evolution  
1001 of surface humidity in Spain: recent trends and possible physical mechanisms. *Clim. Dyn.*  
1002 **42**, 2655-2674, doi:10.1007/s00382-013-1885-7.

1003 Wan, H., X. Zhang, F. W. Zwiers, and H. Shiogama, 2013: Effect of data coverage on the  
1004 estimation of mean and variability of precipitation at global and regional scales. *J.*  
1005 *Geophys. Res. Atmos.*, **118**, 534–546. doi: 10.1002/jgrd.50118

1006 Westra, S., L. V. Alexander, and F. W. Zwiers, 2013: Global increasing trends in annual  
1007 maximum daily precipitation. *J. Climate*, **26**, 3904–3918, doi:10.1175/JCLI-D-12-  
1008 00502.1.

1009 Westra, S., H.J. Fowler, J.P. Evans, L.V. Alexander, P. Berg, F. Johnson, E.J. Kendon, G.  
1010 Lenderink, and N.M. Roberts, 2014: Future changes to the intensity and frequency of  
1011 short-duration extreme rainfall. *Reviews of Geophysics*, DOI: 10.1002/2014RG000464.

1012 WHO/UNICEF Joint Monitoring Programme for Water Supply and Sanitation (JMP),  
1013 2011: Drinking Water Equity, Safety and sustainability: Thematic report on drinking  
1014 water. Available at:  
1015 [www.wssinfo.org/fileadmin/user\\_upload/resources/report\\_wash\\_low.pdf](http://www.wssinfo.org/fileadmin/user_upload/resources/report_wash_low.pdf).

1016 Wilcox, L. J., E. J. Highwood, and N. J. Dunstone, 2013: Influence of aerosol on multi-  
1017 decadal variations of historical global climate. *Environ. Res. Lett.* **8** 024033,  
1018 doi:10.1088/1748-9326/8/2/024033.

1019 Willett, K. M., N. P. Gillett, P. D. Jones and P. W. Thorne, 2007: Attribution of observed  
1020 surface humidity changes to human influence. *Nature*, **449**, 710-712.

1021 Willett, K. W., Jones, P. D, Thorne, P. W. and Gillett, N. P., 2010: A comparison of large  
1022 scale changes in surface humidity over land in observations and CMIP3 GCMs. *Environ.*  
1023 *Res. Lett.*, **5**, 025210, doi: 10.1088/1748-9326/5/2/025210.

1024 Willett, K. M., Williams Jr., C. N., Dunn, R. J. H., Thorne, P. W., Bell, S., de Podesta, M.,  
1025 Jones, P. D., and Parker D. E., 2013: HadISDH: An updated land surface specific humidity  
1026 product for climate monitoring. *Climate of the Past*, **9**, 657-677, doi:10.5194/cp-9-657-  
1027 2013.

1028 Willett, K. M., D. I. Berry and A. Simmons, 2014: Surface Humidity [in .State of the  
1029 Climate in 2013.]. *Bull. Amer. Meteor. Soc.*, **95**, S19-S20.

1030 Winterrath, T., Reich, T., Rosenow, W. and K. Stephan, 2012a: The DWD Quantitative  
1031 Precipitation Nowcasting Systems – A Verification Study for Selected Flood Events. *Proc.*  
1032 *7th Europ. Conf. On Radar in Meteor. and Hydrol.* , Toulouse, France.

- 1033 Winterrath, T., E. Weigl, M. Hafer, and A. Becker, 2012b: D. Wetterdienst, *Proc. 7th*  
1034 *Europ. Conf. On Radar in Meteor. and Hydrol.*, Toulouse, France.
- 1035 World Water Development Report, 2003: *Water for people, water for life*. United Nations  
1036 Educational, Scientific and Cultural Organization and Berghahn Books. ISBN  
1037 UNESCO:92-3-103881-8, ISBN Berghahn: 1-57181-627-5.
- 1038 Wu, P., R. Wood, and J. Ridley, 2010: Temporary acceleration of the hydrological cycle in  
1039 response to a CO<sub>2</sub> rampdown. *Geophys. Res. Lett.*, **37**, L12705,  
1040 doi:10.1029/2010GL043730.
- 1041 Wu, P., N. Christidis and P. Stott, 2013: Anthropogenic impact on Earth's hydrological  
1042 cycle. *Nature Climate Change*, **3**, 807-810, doi:10.1038/NCLIMATE1932
- 1043 Xie, P., P.A. Arkin, 1998: Global Monthly Precipitation Estimates from Satellite-Observed  
1044 Outgoing Longwave Radiation. *J. Climate*, **11**, 137–164.
- 1045 Xie, S.-P., C. Deser, G.A. Vecchi, J. Ma, H. Teng, and A.T. Wittenberg, 2010: Global  
1046 Warming pattern formation: Sea surface temperature and rainfall. *J. Climate*, **23**, 966-  
1047 986.
- 1048 Yin, J. H., 2005: A consistent poleward shift of the storm tracks in simulations of 21st  
1049 century climate. *Geophys. Res. Lett.*, **32**, L18701, doi:10.1029/2005GL023684.
- 1050 Yu, L., and R. A. Weller, 2007: Objectively Analyzed Air–Sea Heat Fluxes for the Global  
1051 Ice-Free Oceans (1981–2005). *Bull. Amer. Meteor. Soc.*, **88**, 527–539.
- 1052 Yu, L., X. Jin, and R. A. Weller, 2008: Multidecade Global Flux Datasets from the  
1053 Objectively Analyzed Air-sea Fluxes (OAFlux) Project: Latent and sensible heat fluxes,

1054 ocean evaporation, and related surface meteorological variables. Woods Hole  
1055 Oceanographic Institution, *OAFflux Project Technical Report*. OA-2008-01, 64pp. Woods  
1056 Hole. Massachusetts.

1057 Zelinka, M., D., T. Andrews, P. M. Forster, and K. E. Taylor, 2014: Quantifying  
1058 Components of Aerosol-Cloud-Radiation Interactions in Climate Models. *J. Geophys. Res.*,  
1059 **119**, 7599-7615, doi: 10.1002/2014JD021710.2

1060 Zhang, X., F. W. Zwiers FW, G. C. Hegerl, F. H. Lambert, N. P. Gillett, S. Solomon, P. A. Stott,  
1061 and T. Nozawa, 2007: Detection of human influence on twentieth-century precipitation  
1062 trends. *Nature*, **448**, 461–465.

1063 Zhang, X., H. Wan, F. W. Zwiers, G.C. Hegerl, and S.-K. Min, 2013: Attributing  
1064 intensification of precipitation extremes to human influence. *Geophys. Res. Lett.*, **40**,  
1065 5252–5257, doi:10.1002/grl.51010.

1066 Zhao, T., A. Dai, and J. Wang, 2012: Trends in tropospheric humidity from 1970-2008 over  
1067 China from a homogenized radiosonde dataset. *J. Climate*, **25**: 4549-4567.

1068 Zolina, O., C. Simmer, S. K. Gulev, and S. Kollet, 2010: Changing structure of European  
1069 precipitation: longer wet periods leading to more abundant rainfalls. *Geophys. Res. Lett.*,  
1070 **37**, L06704, doi:10.1029/2010GL042468.

1071

1072 **Figure Captions**

1073 **Figure 1 left panel:** Projected global-mean precipitation change (mm/day) against  
1074 global-mean 2m air temperature change (K) from CMIP5 models, for four  
1075 representative concentration pathways (RCP) scenarios. Values are means over  
1076 successive decades between 2006 and 2095 and all ensemble members of each model.  
1077 Anomalies are relative to mean values over 1986-2005 in the CMIP5 historical runs.  
1078 Right panel: Precipitation sensitivity for future (RCP scenarios) and past (Historical and  
1079 Atmospheric Model Intercomparison Project, AMIP) change in precipitation amount [%]  
1080 per degree global-mean warming. Trends are calculated from the linear least squares fit  
1081 of annual global-mean precipitation change (%) against temperature (K) change  
1082 relative to the period 1988-2005 (without decadal smoothing). Crosses indicate  
1083 ensemble means for each CMIP5 model, circles indicate multi-model mean.  
1084 Precipitation sensitivity is also shown for historical periods; comparing GCMs with  
1085 GPCP, GPCC and CRU data (see text), using temperature changes from HadCRUT4  
1086 (Morice et al., 2012; note that land and ocean  $dP/dT$  values use global-mean  
1087 temperature). Whiskers indicate 95% confidence intervals for observed linear trends  
1088 (model trend confidence intervals are not shown, but are often large).

1089 **Figure 2:** Observed and model simulated annual and zonal mean precipitation change  
1090 (%/decade) for: top, observations where they exist over land; bottom, GCMs, all  
1091 gridboxes. Top panel: Observed 1951-2005 changes (solid colored lines) from 4  
1092 datasets CRU TS3.0 updated, Harris et al. 2014; Zhang et al. 2007 updated; GPCC  
1093 VasClim0, Beck et al. 2005; and GPCC Full data V6, Becker et al. 2013). Range of CMIP5  
1094 model simulations (grey shading, masked to cover land only) and multi-model ensemble

1095 mean (black dashes, 'MM'). Blue shading shows latitudes where all observed datasets  
1096 show positive trends and orange shading shows where all show negative trends.  
1097 Interpolated data in the CRU dataset are masked out. Bottom panel: Trends based on  
1098 global coverage from climate models from the Historical simulations (grey dashed lines  
1099 are individual simulations, black dashed line multi-model mean; blue dashes multi-  
1100 model mean from simulations forced by natural forcing only) compared to the 2006-  
1101 2050 trend from the RCP4.5 multimodel simulations (green shading: 5-95% range,  
1102 green dashes: multimodel mean). Blue (orange) shading indicates where more than two  
1103 thirds of the historical simulations show positive (negative) trends.

1104 **Figure 3:** Three observed estimates of long-term global and basin zonal-mean near-  
1105 surface salinity changes, nominally for the 1950-2000 period. Positive values show  
1106 increased salinities and negative values freshening. Changes are expressed on the  
1107 Practical Salinity Scale (PSS-78) per 50-years. The data coverage, as used in Durack and  
1108 Wijffels (2010), is shown in Supplementary Figure 1. Reproduced from Durack et al.  
1109 (2013).

1110 **Figure 4:** Number of in situ stations over time for the CRU TS 3.21 gridded precipitation  
1111 dataset (updated from Harris et al., 2014). Evolution over decades of the latitudinal  
1112 density of stations per zonal band for the Americas (orange), Europe/Africa (green) and  
1113 Asia/Australasia (blue), stacked to indicate the zonal total. Incomplete data series are  
1114 included as a fraction of available data. The black line indicates the number of stations  
1115 per zonal band required to obtain an average zonal coverage of 1 station per  $(100\text{km})^2$   
1116 of land at that latitude. This figure shows the station numbers in absolute terms and in

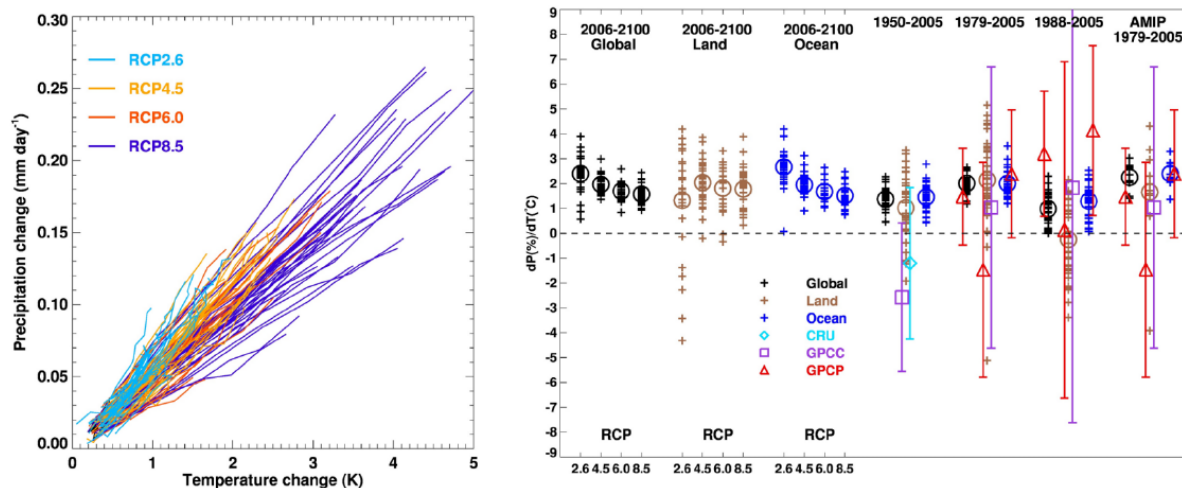
1117 relation to the latitudinally-varying land area. Other datasets have similar differences in  
1118 coverage over time (see supplementary figure 2 for GPCC).

1119 **Figure 5:** High latitude (55-90N) annual mean precipitation trends [mm/decade] from  
1120 1951-2005 for three observational datasets: Zhang et al. (2007; updated; 5x5 degree  
1121 grid); GPCC Full data V6 (Becker et al., 2013), CRU TS3.0, updated (Harris et al., 2013;  
1122 grid points with CRU station data available for >95% of the time are stippled) compared  
1123 to the CMIP5 multimodel mean trend of Historical runs with all external forcings  
1124 ('Multi-model Mean'). Note that both GPCC and CRU use spatial interpolation to varying  
1125 extents, while Zhang et al., 2007 average a subset of stations only, considered to be  
1126 homogeneous in the long-term within grid-boxes.

1127

1128 **Figure 6:** Top: The 2nd EOF of global sea surface temperature (3-yr running mean) data  
1129 from 1920-2011 based on the HadISST data set. The red line is a smoothed index  
1130 representing the inter-decadal Pacific Oscillation (IPO). The bottom panel shows  
1131 smoothed precipitation anomalies averaged over the Southwest U.S. (black line)  
1132 compared with the IPO index, scaled for comparison. (Reproduced from Dai 2013b).

1133

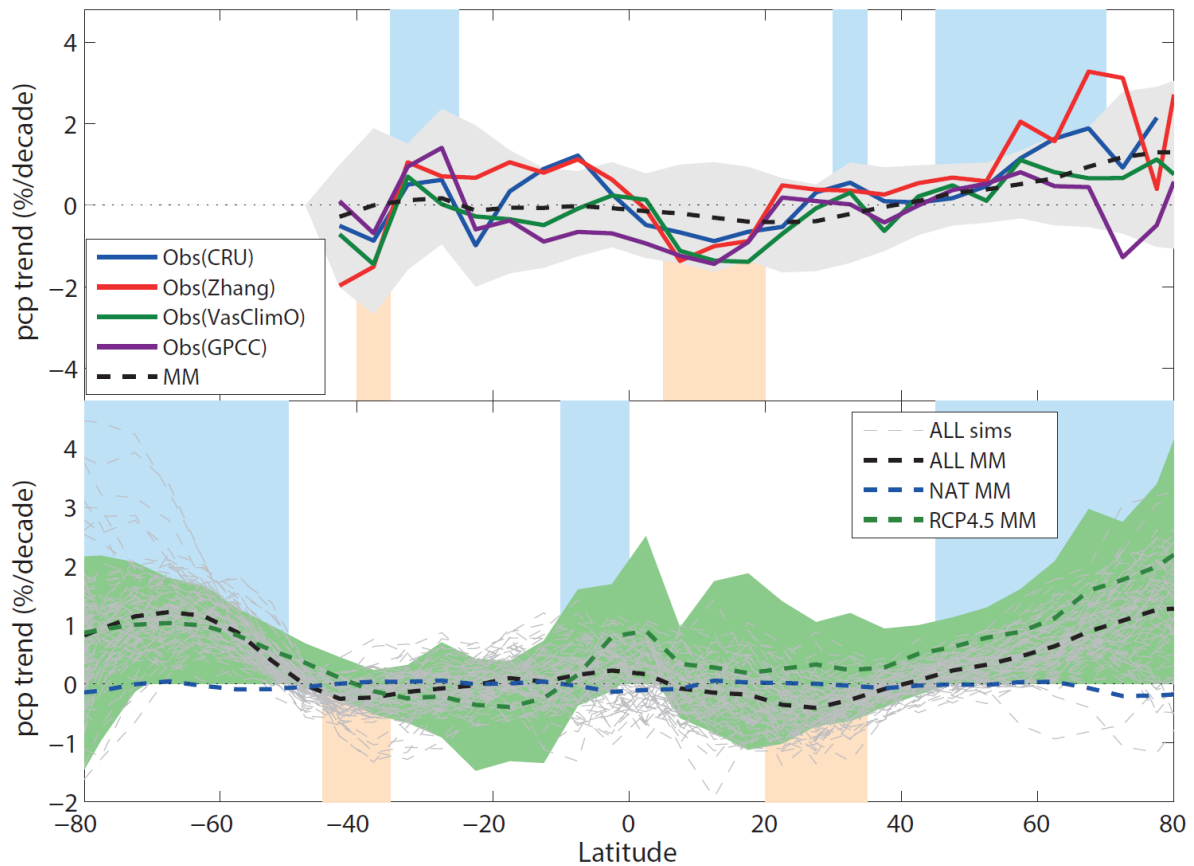


1134

1135 **Figure 1 left panel:** Projected global-mean precipitation change (mm/day) against  
 1136 global-mean 2m air temperature change (K) from CMIP5 models, for four  
 1137 representative concentration pathways (RCP) scenarios. Values are means over  
 1138 successive decades between 2006 and 2095 and all ensemble members of each model.  
 1139 Anomalies are relative to mean values over 1986-2005 in the CMIP5 historical runs.  
 1140 **Right panel:** Precipitation sensitivity for future (RCP scenarios) and past (Historical  
 1141 and Atmospheric Model Intercomparison, AMIP) change in precipitation amount [%]  
 1142 per degree global-mean warming. Trends are calculated from the linear least squares fit  
 1143 of annual global-mean precipitation change (%) against temperature (K) change  
 1144 relative to the period 1988-2005 (without decadal smoothing). Crosses indicate  
 1145 ensemble means for each CMIP5 model, circles indicate multi-model mean.  
 1146 Precipitation sensitivity is also shown for historical periods; comparing GCMs with  
 1147 GPCP, GPCP and CRU data (see text), using temperature changes from HadCRUT4  
 1148 (Morice et al., 2012; note that land and ocean  $dP/dT$  values use global-mean  
 1149 temperature). Whiskers indicate 95% confidence intervals for observed linear trends  
 1150 (model trend confidence intervals are not shown, but are often large).

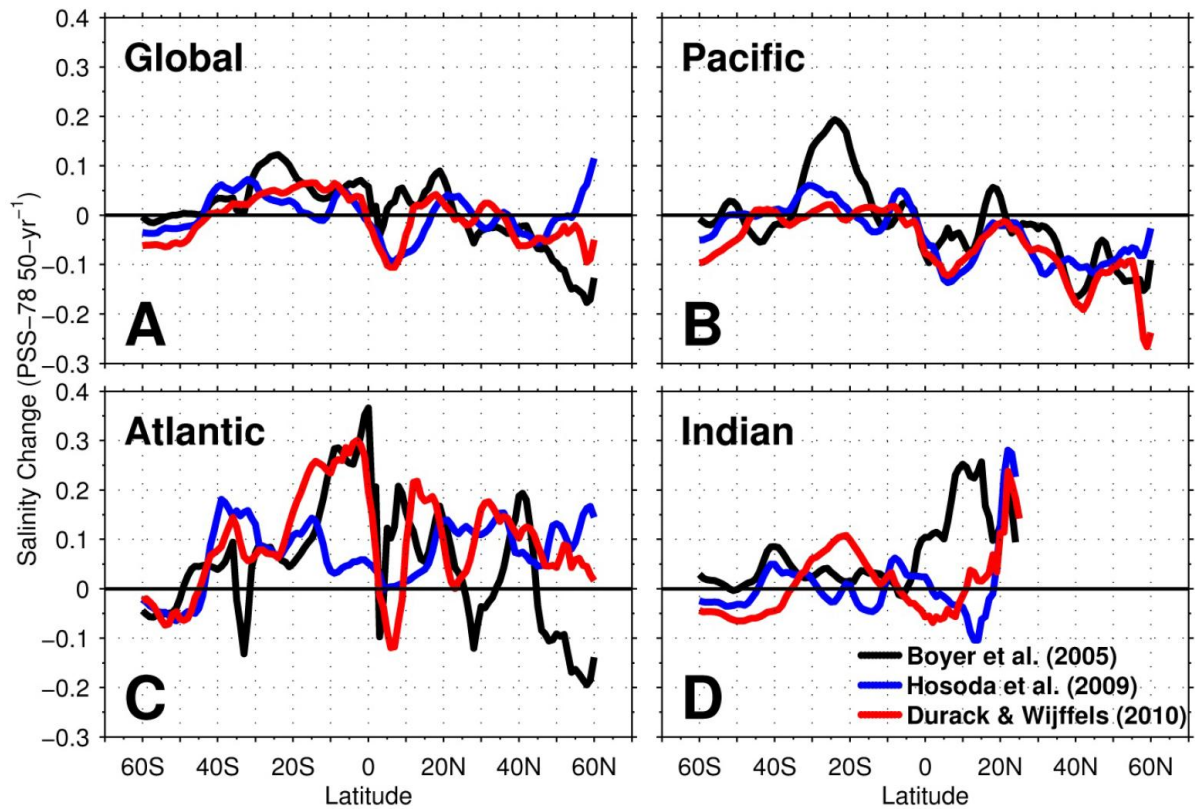
1151





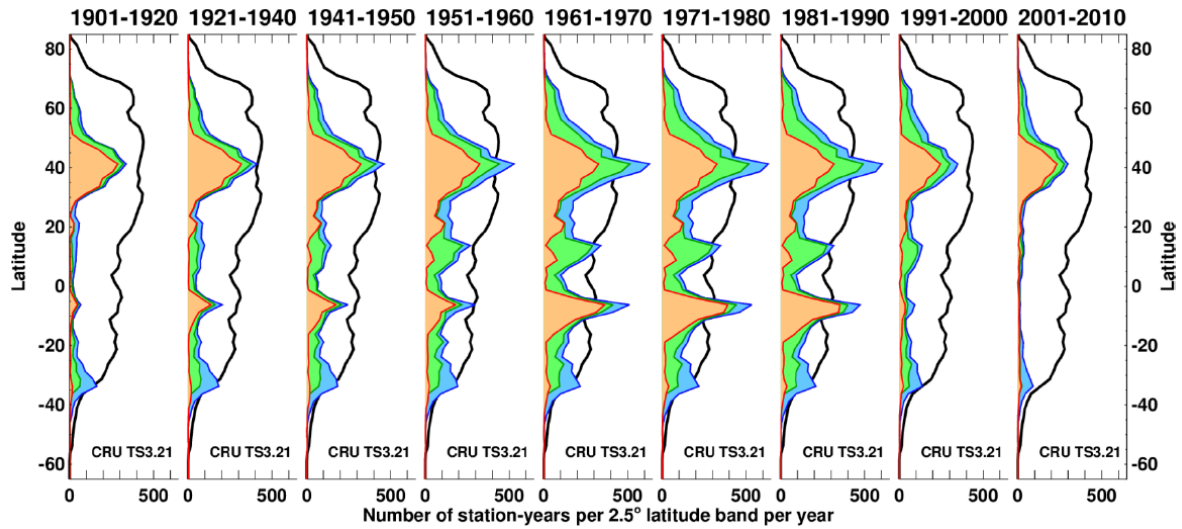
1152

1153 **Figure 2:** Observed and model simulated annual and zonal mean precipitation change  
 1154 (%/decade) for: top, observations where they exist over land; bottom, GCMs, all  
 1155 gridboxes. Top panel: Observed 1951-2005 changes (solid colored lines) from 4  
 1156 datasets CRU TS3.0 updated, Harris et al. 2013; Zhang et al. 2007 updated; GPCC  
 1157 VasClimO, Beck et al. 2005; and GPCC Full data V6, Becker et al. 2013). Range of CMIP5  
 1158 model simulations (grey shading, masked to cover land only) and multi-model ensemble  
 1159 mean (black dashes, 'MM'). Blue shading shows latitudes where all observed datasets  
 1160 show positive trends and orange shading shows where all show negative trends.  
 1161 Interpolated data in the CRU dataset are masked out. Bottom panel: Trends based on  
 1162 global coverage from climate models from the Historical simulations (grey dashed lines  
 1163 are individual simulations, black dashed line multi-model mean; blue dashes multi-  
 1164 model mean from simulations forced by natural forcing only) compared to the 2006-  
 1165 2050 trend from the RCP4.5 multimodel simulations (green shading: 5-95% range,  
 1166 green dashes: multimodel mean). Blue (orange) shading indicates where more than two  
 1167 thirds of the historical simulations show positive (negative) trends.



1168  
 1169 **Figure 3:** Three observed estimates of long-term global and basin zonal-mean near-  
 1170 surface salinity changes, nominally for the 1950-2000 period. Positive values show  
 1171 increased salinities and negative values freshening. Changes are expressed on the  
 1172 Practical Salinity Scale (PSS-78) per 50-years. The data coverage, as used in Durack and  
 1173 Wijffels (2010), is shown in Supplementary Figure 1. Reproduced from Durack et al.  
 1174 (2013).

1175



1177

1178

1179

1180

1181

1182

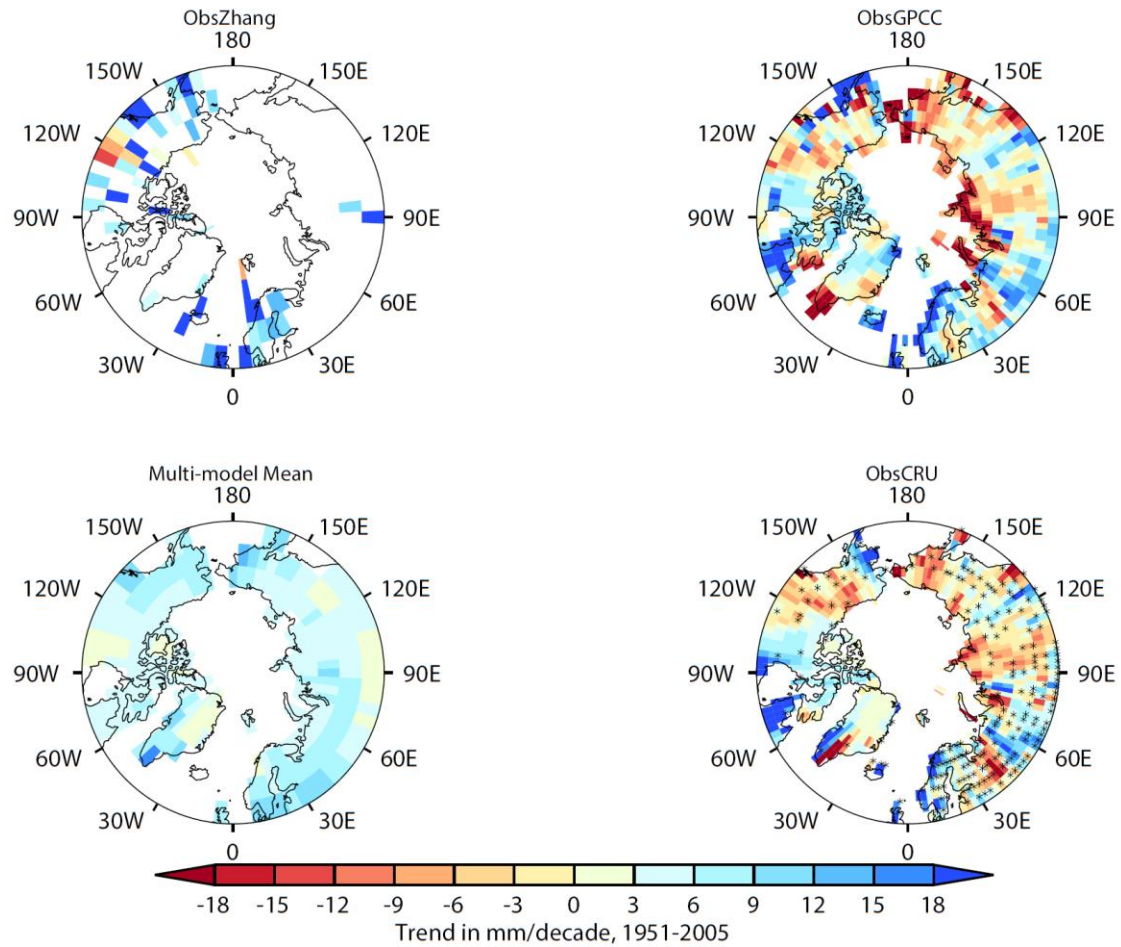
1183

1184

1185

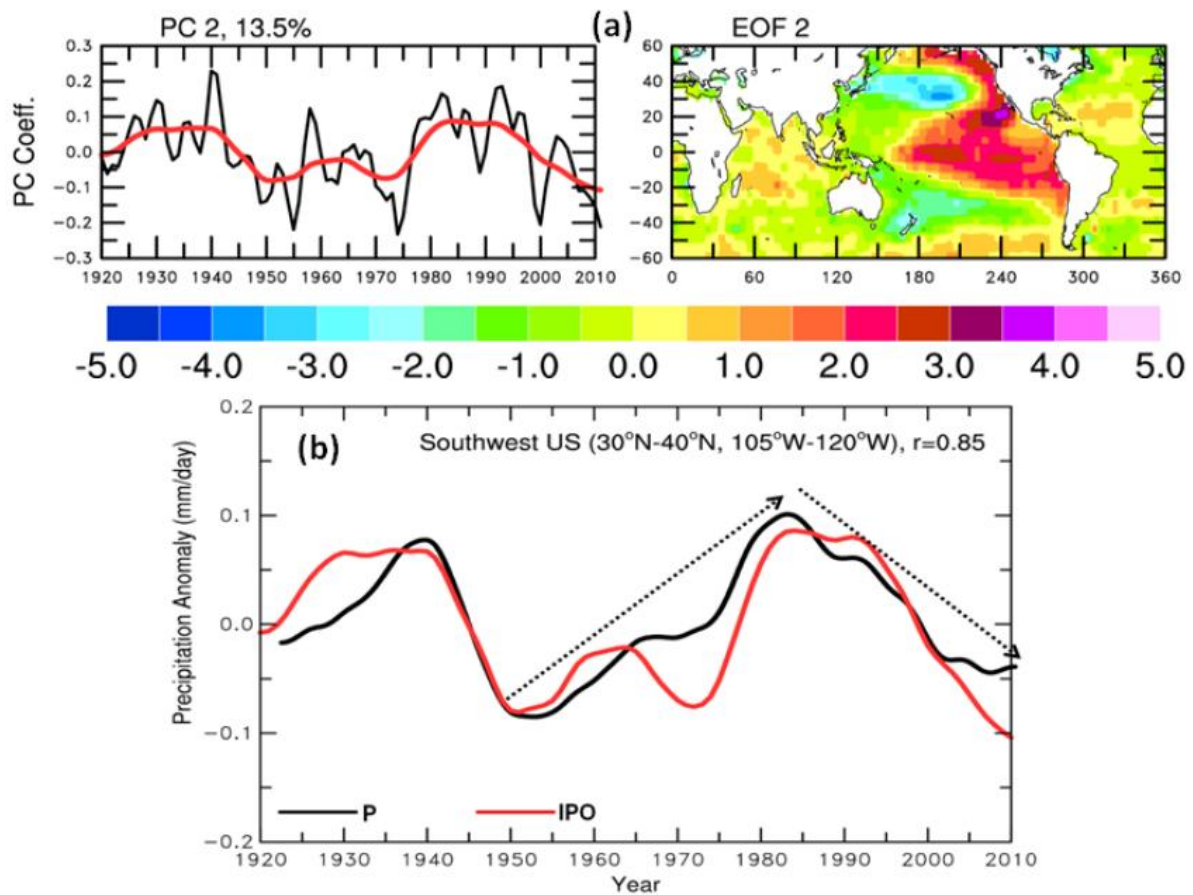
1186

**Figure 4:** Number of in situ stations over time for the CRU TS 3.21 gridded precipitation dataset (updated from Harris et al., 2013). Evolution over decades of the latitudinal density of stations per zonal band for the Americas (orange), Europe/Africa (green) and Asia/Australasia (blue), stacked to indicate the zonal total. Incomplete data series are included as a fraction of available data. The black line indicates the number of stations per zonal band required to obtain an average zonal coverage of 1 station per  $(100\text{km})^2$  of land at that latitude. This figure shows the station numbers in absolute terms and in relation to the latitudinally-varying land area. Other datasets have similar differences in coverage over time (see supplementary figure 2 for GPCC).



1187

1188 **Figure 5:** High latitude (55-90N) annual mean precipitation trends [mm/decade] from  
 1189 1951-2005 for three observational datasets: Zhang et al. (2007; updated; 5x5 degree  
 1190 grid); GPCC Full data V6 (Becker et al., 2013), CRU TS3.0, updated (Harris et al., 2013;  
 1191 grid points with CRU station data available for >95% of the time are stippled) compared  
 1192 to the CMIP5 multimodel mean trend of Historical runs with all external forcings  
 1193 ('Multi-model Mean'). Note that both GPCC and CRU use spatial interpolation to varying  
 1194 extents, while Zhang et al., 2007 average a subset of stations only, considered to be  
 1195 homogeneous in the long-term within grid-boxes.



1196

1197 **Figure 6:** Top: The 2nd EOF of global sea surface temperature (3-yr running mean) data  
 1198 from 1920-2011 based on the HadISST data set. The red line is a smoothed index  
 1199 representing the inter-decadal Pacific Oscillation (IPO). The bottom panel shows  
 1200 smoothed precipitation anomalies averaged over the Southwest U.S. (black line)  
 1201 compared with the IPO index, scaled for comparison. (Reproduced from Dai 2013b).

1202

1203